

Photon-assisted electron transport through a three-terminal quantum dot system with nonresonant tunneling channels

T. Kwapiński,* R. Taranko,[†] and E. Taranko[‡]

*Institute of Physics, Maria Curie-Skłodowska University and Maria Curie-Skłodowska University Nanotechnology Center,
20-031 Lublin, Poland*

(Received 2 March 2005; revised manuscript received 12 July 2005; published 8 September 2005)

We have studied the electron transport through a quantum dot coupled to three leads in the presence of external microwave fields supplied to different parts of the considered mesoscopic system. Additionally, we introduced a possible nonresonant tunneling channel between leads. The quantum dot charge and currents were determined in terms of the appropriate evolution operator matrix elements and under the wide-band limit the analytical formulas for time-averaged currents and differential conductance were obtained. We have also examined the response of the considered system on the rectangular-pulse modulation imposed on different quantum dot-lead barriers as well as the time dependence of currents flowing in response to suddenly removed (or included) connection of a quantum dot with one of the leads.

DOI: [10.1103/PhysRevB.72.125312](https://doi.org/10.1103/PhysRevB.72.125312)

PACS number(s): 73.23.-b, 73.63.Kv

I. INTRODUCTION

The electron transport via resonant tunneling in mesoscopic systems has been the subject of extensive theoretical research due to recent development in fabrication of small electronic devices and their potential applications. Some interest has been focused on the transport properties of a quantum dot (QD) under the influence of external time-dependent fields. Interesting effects have been observed and theoretically described, e.g., photon-assisted tunneling through small quantum dots,^{1,2} photon-electron pumps³ and others. In most theoretical investigations a QD placed between two leads was considered (e.g., Refs. 2 and 4–9) and the current flowing through a QD under periodic modulation of the QD electronic structure or periodic (nonperiodic) modulation of the tunneling barriers and electron energy levels of both (left and right) leads was calculated.

One of the important problems of the mesoscopic physics is the interference of the charge carriers. This interference appears when two (or more) transmission channels for electron tunneling exist. Such possibility exists, e.g., in the electron transport through a QD embedded in a ring in the Aharonov-Bohm geometry and much theoretical interest has been paid to description of the phase coherence in this and related systems, e.g., Refs. 10–12. Another experimental situation in which the interference may occur can be realized with the scanning tunneling microscope (STM). The recent experimental and theoretical studies with a low-temperature STM of a single atom deposited on a metallic surface showed the asymmetric Fano resonances in the tunneling spectra, e.g., Refs. 13 and 14. In the STM measurements the tip probes the transmission of electrons either through the adsorbed atom or directly from the surface. The transport of electrons through both channels leads to an asymmetric shape of the conductance curves which is typical behavior for the Fano resonance resulting from constructive and destructive interference processes. The quantum interference can be also observed in the mesoscopic system with multiple energy levels.¹⁵ A model which incorporates a weak direct

nonresonant transmission through a QD as well as the resonant tunneling channel was also considered in Ref. 16 in the context of the large value of the transmission phase found in the experiment for the Kondo regime of a QD.¹⁷

A number of works have been devoted to the problem of the electron transport in the multiterminal QD systems and here we mention only a few of them. In Ref. 18 the conductance of the N -lead system was considered showing that the Kondo resonance at equilibrium is split into $N-1$ peaks. In Ref. 19 an explicit form for the transmission coefficient in the electron transport through a QD connected with three leads was found. The electron transport and shot noise in a multiterminal coupled QD system in which each lead was disturbed by classical microwave fields were studied in Ref. 20. Multiterminal QD systems or magnetic junctions were also intensively investigated in context of the spin-dependent transport, e.g., Refs. 21 and 22. The general formulation of the time-dependent spin-polarized transport in a system consisting of the resonant tunneling structure coupled with several magnetic terminals was considered by Zhu *et al.*²² and as an application of this formalism the electron transport in a system with two terminals under an ac external field was investigated. A three-terminal QD system was studied in Refs. 23 and 24 to measure the nonequilibrium QD density of states (splitting of the Kondo resonance peak). The cross correlations of the currents and the differential conductance of the QD coupled with three leads described by the infinite- U Anderson Hamiltonian were considered in Ref. 25; see also Ref. 26. A mesoscopic sample connected to many reservoirs via single channel leads was considered in Ref. 27 in the context of the quantum pump effect. The transport properties of molecule wires or coupled quantum dots placed between three leads and irradiated by the infrared light quanta were studied in Ref. 28 and the possibility of controlling the currents flowing in the system was discussed.

In all papers mentioned above and relating to the studies of the electron transport through a two-terminal QD with the additional (bridge) nonresonant transmission channel, the time-dependent external fields were not applied and the con-

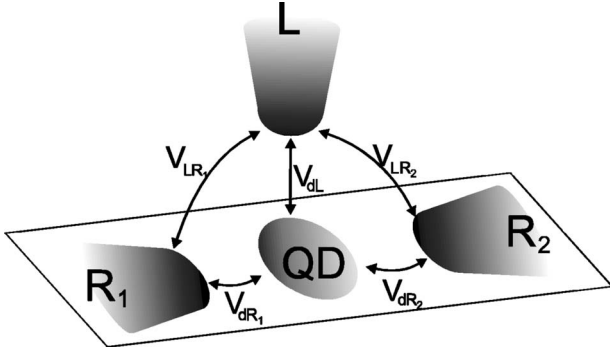


FIG. 1. Schematic picture of the QD coupled with three leads. It can serve as a possible STM experimental setup when the L lead corresponds to the STM tip.

considered systems were driven out of the equilibrium only by means of a dc voltage bias (see, however, Ref. 29). On the other hand, in papers considering the multiterminal QD systems in the presence of the external microwave fields, the nonresonant tunneling channels between different leads were not considered.

In this paper, we address the issue of a QD coupled with three leads with additional, nonresonant coupling between leads driven out of equilibrium by means of a dc voltage bias and time-dependent external fields. The QD is connected with three metal leads and one of these leads, say the left (L) lead, is coupled with the two remaining leads, say the first (R_1) and the second (R_2) right leads. The one possible experimental setup (e.g., in the STM measurement) corresponding to our model system is presented in Fig. 1. We have decided to denote the three leads by the subscripts L , R_1 , and R_2 in order to have the simplified comparison with the two-terminal QD systems described in literature (usually presented as left lead–QD–right lead). In literature, different theoretical approaches have been developed to treat the time-dependent electron transport in the mesoscopic systems. The most popular nonequilibrium Green’s-function method depends on the two time arguments and for time-dependent problems it is a rather difficult task to calculate them without any approximations (e.g., beyond the wide-band limit). Therefore in our treatment of the time-dependent problems we use the evolution operator which, as a rule, essentially depends on one time argument (e.g., Refs. 30–32). Such an approach is especially well suited for the problem with time-dependent coupling between the QD and leads, see also Ref. 33 where the evolution operator method was used in a detailed investigation of the zero-frequency noise and time-dependent current in a mesoscopic system irradiated by the laser radiation or microwave field.

The outline of the paper is as follows. In Secs. II and III we start with the model and method for the derivation of the QD charge and currents. In Sec. IV we present the results for the time-averaged currents and their derivatives with respect to the QD energy level position (or equivalently, with respect to the gate voltage) obtained for different time dependence of the parameters characterizing the considered system. We consider also the transient current characteristics in the case of the rectangular-pulse modulations imposed on the QD-

lead barriers. The last section presents the conclusions and in the Appendix we give the short derivation of the evolution operator matrix elements needed in the QD charge and current calculations.

II. MODEL AND GENERAL FORMULATION

We consider a QD coupled through the tunneling barriers $V_{\vec{k}_i d}$ ($i=1,2,3$) to three metal leads. One of these leads, say the left lead (L) is coupled additionally with the remaining two leads, say the first and second right leads (R_1, R_2) by the tunneling barriers $V_{\vec{k}_L, \vec{k}_R}$. In the following we will denote the wave vectors associated with the left lead by the letter \vec{k} and the wave vectors corresponding to the first and second right leads by the letters \vec{q} and \vec{r} , respectively. The chemical potentials μ_i of the three metal leads may not be equal, and their difference is not necessarily small. We write the Hamiltonian of the considered system in the form $H=H_0+V$, where

$$H_0 = \sum_{\vec{p}=\vec{k}, \vec{r}, \vec{q}} \varepsilon_{\vec{p}}(t) a_{\vec{p}}^{\dagger} a_{\vec{p}} + \varepsilon_d(t) a_d^{\dagger} a_d, \quad (1)$$

$$V = \sum_{\vec{p}=\vec{k}, \vec{r}, \vec{q}} [V_{\vec{p}d}(t) a_{\vec{p}}^{\dagger} a_d + \text{H. c.}] + \sum_{\vec{k}, \vec{r}} [V_{\vec{k}\vec{r}}(t) a_{\vec{k}}^{\dagger} a_{\vec{r}} + \text{H. c.}] \\ + \sum_{\vec{k}, \vec{q}} [V_{\vec{k}\vec{q}}(t) a_{\vec{k}}^{\dagger} a_{\vec{q}} + \text{H. c.}]. \quad (2)$$

The operators $a_{\vec{p}}(a_{\vec{p}}^{\dagger})$, $a_d(a_d^{\dagger})$ are the annihilation (creation) operators of the electrons in the corresponding leads and the dot, respectively. For simplicity the dot is characterized only by a single level ε_d and the intradot electron-electron Coulomb interaction is neglected. The neglect of Coulomb interaction is quite reasonable in some situations and, as we are going to concentrate on the investigations of the influence of the third lead (in comparison with the QD–two leads system) and the additional tunneling channels between the leads on the time-dependent transport, then in the first step we ignore the Coulomb interaction. We obtain, for example, as the one of the consequences of neglecting of intradot Coulomb interaction, the average current vs the QD energy level in the form of a single peak instead of a series of oscillation peaks. However, as the experiment indicates, e.g., Ref. 3, each of these peaks is modified in a similar manner by the external time-dependent field, so our analysis of one of these peaks should be justified. We consider our mesoscopic system in the presence of external microwave fields which are applied to the dot and three leads. In most theoretical treatments of photon-assisted electron tunneling it is assumed that the driving field equals the applied external field. However, the situation is more complicated and the internal potential can be different from the applied potential. One of the consequences will be, e.g., the asymmetry between the corresponding left and right sidebands.³⁴ The main feature of the time-dependent transport remains, however, unchanged and in our treatment as usual we assume that in the adiabatic approximation the energy levels of the leads and QD are driven with the frequency ω and the amplitudes Δ_i ($i=L, R_1, R_2$), Δ_d and read $\varepsilon_{\vec{k}_i}(t) = \varepsilon_{\vec{k}_i} + \Delta_i \cos \omega t$, $\varepsilon_d(t) = \varepsilon_d + \Delta_d \cos \omega t$, respectively.

The time evolution of the QD charge and the current flowing in the system can be described in terms of the time-evolution operator $U(t, t_0)$ given by the equation of motion (in the interaction representation)

$$i \frac{\partial U(t, t_0)}{\partial t} = \tilde{V}(t)U(t, t_0), \quad (3)$$

with $\tilde{V}(t) = U_0(t, t_0)V(t)U_0^\dagger(t, t_0)$ and $U_0(t, t_0) = T \exp[i \int_{t_0}^t dt_1 H_0(t_1)]$ where T denotes the time ordering and the units such that $\hbar=1$ have been chosen. Here we have assumed that the interactions between the QD and leads, as well as between the left and right leads, are switched on in the distant past t_0 .

The QD charge (in units of e) is calculated according to the formula (cf. Refs. 30 and 31)

$$n_d(t) = n_d(t_0) |U_{dd}(t, t_0)|^2 + \sum_{\vec{p}=\vec{k}, \vec{q}, \vec{r}} n_{\vec{p}}(t_0) |U_{d\vec{p}}(t, t_0)|^2. \quad (4)$$

Here $U_{dd}(t, t_0)$ and $U_{d\vec{p}}(t, t_0)$ denote the matrix elements of the evolution operator calculated within the basis functions containing the single-particle functions $|\vec{k}\rangle$, $|\vec{q}\rangle$, $|\vec{r}\rangle$, and $|d\rangle$ corresponding to three leads and QD, respectively. $n_d(t_0)$ and $n_{\vec{p}}(t_0)$ represent the initial filling of the corresponding single-particle states.

The tunneling current flowing, e.g., from the left lead $j_L(t)$, can be obtained using the time derivative of the total number of electrons in the left lead, $j_L(t) = -e dn_L(t)/dt$, where

$$n_L(t) = \sum_{\vec{k}} n_{\vec{k}}(t) = \sum_{\vec{k}} n_d(t_0) |U_{\vec{k}d}(t, t_0)|^2 + \sum_{\vec{k}, \vec{k}_1} n_{\vec{k}_1}(t_0) |U_{\vec{k}\vec{k}_1}(t, t_0)|^2 + \sum_{\vec{k}, \vec{q}} n_{\vec{q}}(t_0) |U_{\vec{k}\vec{q}}(t, t_0)|^2 + \sum_{\vec{k}, \vec{r}} n_{\vec{r}}(t_0) |U_{\vec{k}\vec{r}}(t, t_0)|^2. \quad (5)$$

In the following only the matrix elements of the evolution operator present in Eqs. (4) and (5) are required and they can be obtained solving the corresponding sets of coupled differential equations constructed according to Eq. (3) with $\tilde{V}_{ab}(t)$ written as follows:

$$\tilde{V}_{ab}(t) = V_{ab}(t) \exp \left(i(\varepsilon_a - \varepsilon_b)(t - t_0) + i \frac{\Delta_a - \Delta_b}{\omega} (\sin \omega t - \sin \omega t_0) \right), \quad (6)$$

where a and b correspond to $|\vec{k}\rangle$, $|\vec{q}\rangle$, $|\vec{r}\rangle$, or $|d\rangle$, respectively.

As the example, the matrix element $U_{dd}(t, t_0)$ required for the calculation of the first term of the QD charge, Eq. (4), can be obtained solving the following set of coupled differential equations:

$$\frac{\partial U_{dd}(t, t_0)}{\partial t} = -i \sum_{\vec{p}=\vec{k}, \vec{q}, \vec{r}} \tilde{V}_{d\vec{p}}(t) U_{\vec{p}d}(t, t_0), \quad (7)$$

$$\frac{\partial U_{\vec{k}d}(t, t_0)}{\partial t} = -i \tilde{V}_{\vec{k}d}(t) U_{dd}(t, t_0) - i \sum_{\vec{p}=\vec{q}, \vec{r}} \tilde{V}_{\vec{k}\vec{p}}(t) U_{\vec{p}d}(t, t_0), \quad (8)$$

$$\frac{\partial U_{\vec{p}d}(t, t_0)}{\partial t} = -i \tilde{V}_{\vec{p}d}(t) U_{dd}(t, t_0) - i \sum_{\vec{k}} \tilde{V}_{\vec{p}\vec{k}}(t) U_{\vec{k}d}(t, t_0), \quad (9)$$

$$\vec{p} = \vec{q}, \vec{r}.$$

The total number of coupled equations in this case is equal to $(3N+1)$, N being the number of discrete wave vectors \vec{k} , \vec{q} , and \vec{r} taken to perform the corresponding summation over the wave vectors. In the calculations the summations over wave vectors were replaced, as usual, with integrations over energy weighted with a given lead density of states (taken as a constant value). Usually, $N=100-200$ wave vectors, or equivalently 100–200 energy points uniformly distributed along the lead energy band, is sufficient to achieve the desired accuracy of the calculations. We have solved numerically this and other similar sets of the coupled differential equations needed in calculations of all matrix elements of the evolution operator present in Eqs. (4) and (5). We have used this method for the special case of time-dependent couplings of the QD with leads and the couplings of the left lead with two right leads. The set of Eqs. (7)–(9) in the case of vanishing overdot couplings between the left and right leads is greatly simplified and gives, e.g., for $U_{dd}(t, t_0)$,

$$\frac{\partial U_{dd}(t, t_0)}{\partial t} = - \int_{t_0}^t dt_1 K(t, t_1) U_{dd}(t, t_0), \quad (10)$$

where

$$K(t, t_1) = \sum_{\vec{p}=\vec{k}, \vec{q}, \vec{r}} \tilde{V}_{d\vec{p}}(t) \tilde{V}_{\vec{p}d}(t_1) = \sum_{i=L, R_1, R_2} |V_i|^2 u_i(t) u_i(t_1) D_i(t - t_1) \exp[i\varepsilon_d(t - t_1)] \times \exp[i(\Delta_d - \Delta_i)(\sin \omega t - \sin \omega t_1)/\omega] \quad (11)$$

and $D_i(t - t_1)$ is the Fourier transform of the i th lead density of states and $V_{di}(t) = V_i u_i(t)$. Similar simplifications occur in the calculations of other matrix elements of $U(t, t_0)$ required in the formulas for $n_d(t)$ and $n_L(t)$. However, for the nonvanishing couplings $V_{\vec{k}\vec{q}}$ and $V_{\vec{k}\vec{r}}$ (overdot bridge between the left and right leads) one has to solve the starting set of Eqs. (7)–(9).

III. ELECTRON TRANSPORT IN THE WIDE-BAND LIMIT

Much more analytical calculations can be done in the case of constant values of the tunneling matrix elements present in our model. In this case the general equation satisfied by $U_{dd}(t, t_0)$ is derived in the Appendix [see Eq. (A5)] and under the wide-band limit (WBL) approximation, e.g., Refs. 2, 4, and 5, this equation takes the simple form

$$\frac{\partial U_{dd}(t, t_0)}{\partial t} = -C_1 U_{dd}(t, t_0), \quad (12)$$

here $C_1 = [\frac{3}{2} - (3x^2 + 2ix)/(1 + 2x^2)]\Gamma$, $x = \pi V_{RL}/D$, D being the bandwidth of the lead energy band ($D_{R_1} = D_{R_2} = D_L = D$) and $\Gamma = 2\pi V^2/D$. In the Appendix we give the derivations of all functions needed for calculation of the QD charge and currents. We assumed the simplified assumption that all tunneling matrix elements are independent of the wave vectors. The interactions between the QD and leads are assumed to be equal between themselves and denoted by V and the interactions between the left and two rights leads (i.e., $V_{\vec{k}\vec{q}}$ and $V_{\vec{k}\vec{r}}$) corresponding to the overdot tunneling channels are also equal with one another and denoted by V_{LR} .

It is easy to show that the first term of the general formula for the QD charge, Eq. (4), together with the solution of Eq. (12), $U_{dd}(t, t_0) = \exp[-C_1(t - t_0)]$, tends to zero for $t - t_0 \rightarrow \infty$ as $\text{Re } C_1 = 3\Gamma/2 - 3x^2\Gamma/(1 + 2x^2) > 0$. The next terms of the QD charge formula can be calculated using the functions $U_{d\vec{k}}(t, t_0)$, $U_{d\vec{q}}(t, t_0)$, and $U_{d\vec{r}}(t, t_0)$, Eqs. (A13) and (A17) being the solutions of the corresponding differential equations, Eqs. (A12) and (A16). Finally, the time-averaged QD charge (in units of e) is given by

$$\langle n_d(t) \rangle = \sum_{i=L, R_1, R_2} a_i \int d\varepsilon f_i(\varepsilon) \langle |A_i(\varepsilon, t)|^2 \rangle, \quad (13)$$

where

$$a_L = (1 + 4x^2)/(1 + 2x^2)^2 \Gamma/2\pi, \quad (14)$$

$$a_{R_1} = a_{R_2} = (1 + x^2)/(1 + 2x^2)^2 \Gamma/2\pi, \quad (15)$$

$$\begin{aligned} A_i(\varepsilon, t) = & -i \int_{t_0}^t dt_1 \exp \left[-i(\varepsilon_d - \varepsilon)(t - t_1) - i(\Delta_d - \Delta_i) \right. \\ & \left. \times (\sin \omega t - \sin \omega t_1)/\omega \right] \exp \left(\frac{\Gamma(-3 + i4x)}{2(1 + 2x^2)}(t - t_1) \right). \end{aligned} \quad (16)$$

Here $\langle \dots \rangle$ denotes the time averaging and $f_i(\varepsilon)$ denotes the Fermi function of the i th ($i=L, R_1, R_2$) lead. Noticing that $\text{Im} \langle A_i(\varepsilon, t) \rangle = -[3\Gamma/2/(1 + 2x^2)] \langle |A_i(\varepsilon, t)|^2 \rangle$ (cf. Ref. 5), the expression for the time-averaged QD charge can be written as

$$\begin{aligned} \langle n_d(t) \rangle = & -\text{Im} \left(\frac{1 + 4x^2}{3\pi(1 + 2x^2)} \int f_L(\varepsilon) \langle A_L(\varepsilon, t) \rangle d\varepsilon \right. \\ & \left. + \frac{1 + x^2}{3\pi(1 + 2x^2)} \sum_{i=1,2} \int f_{R_i}(\varepsilon) \langle A_{R_i}(\varepsilon, t) \rangle d\varepsilon \right). \end{aligned} \quad (17)$$

In order to calculate the current $j_L(t)$ the functions $U_{\vec{k}d}(t, t_0)$, $U_{\vec{k}_1\vec{k}_2}(t, t_0)$, $U_{\vec{k}\vec{q}}(t, t_0)$, and $U_{\vec{k}\vec{r}}(t, t_0)$ are required and they are given in the Appendix in Eqs. (A7), (A14), and (A19). After lengthly but straightforward calculations we obtain for the time-averaged current leaving the left lead the following formula:

$$\begin{aligned} \langle j_L(t) \rangle = & \frac{e}{\hbar} \sum_{i=R_1, R_2} \text{Re} \left[\frac{2x^2}{\pi(1 + 2x^2)^2} (\mu_L - \mu_i) \right. \\ & \left. + G \left(\int f_L(\varepsilon) \langle A_L(\varepsilon, t) \rangle d\varepsilon - \int f_i(\varepsilon) \langle A_i(\varepsilon, t) \rangle d\varepsilon \right) \right], \end{aligned} \quad (18)$$

where

$$G = \frac{\Gamma}{3\pi(1 + 2x^2)^3} [6x(1 - 2x^2) + i(1 - 13x^2 + 4x^4)], \quad (19)$$

$$\begin{aligned} \langle A_j(\varepsilon, t) \rangle = & \sum_k J_k^2 \left(\frac{\Delta_d - \Delta_j}{\omega} \right) \\ & \times \left(\varepsilon - \varepsilon_d - \omega k + \frac{2\Gamma x}{1 + 2x^2} + i \frac{3\Gamma/2}{1 + 2x^2} \right)^{-1}, \end{aligned} \quad (20)$$

and $J_k(y)$ denotes the Bessel function. The corresponding formula for the time-averaged current $\langle j_{R_i}(t) \rangle$ leaving the R_i lead, $i=1,2$, cannot be written in such symmetrical form as in Eq. (18), because the R_i lead is coupled with the L lead only. For $\langle j_{R_i}(t) \rangle$ we have

$$\begin{aligned} \langle j_{R_i}(t) \rangle = & \frac{e}{\hbar} \text{Re} \left[\frac{2x^2}{\pi(1 + x^2)^2} [\mu_{R_i} - \mu_L + x^2(\mu_{R_i} - \mu_{R_j})] \right. \\ & + \frac{\Gamma}{3\pi(1 + 2x^2)^3} \left(2G_2 \int f_{R_i}(\varepsilon) \langle A_{R_i}(\varepsilon, t) \rangle d\varepsilon \right. \\ & - G_1 \int f_L(\varepsilon) \langle A_L(\varepsilon, t) \rangle d\varepsilon - G_3 \int f_{R_j}(\varepsilon) \\ & \left. \left. \times \langle A_{R_j}(\varepsilon, t) \rangle d\varepsilon \right) \right], \end{aligned} \quad (21)$$

where $G_1 = 6x(1 - 2x^2) + i(1 - 13x^2 + 4x^4)$, $G_2 = 3x - (i/2)(-2 + 5x^2 + x^4)$, $G_3 = 12x^3 + i(1 + 8x^2 - 5x^4)$ and $j=1(2)$ for $l=2(1)$. Note that the integrals present in the formula for the QD charge and currents, Eqs. (17), (18), and (21) can be easily performed analytically and final algebraic expressions can be obtained. Especially simple and transparent form can be given for the conductance $(\partial/\partial\mu_i) \langle j_j(t) \rangle$, $i, j=L, R_1, R_2$. For example, $\partial \langle j_L(t) \rangle / \partial \mu_L$ reads as (for the temperature $T=0$)

$$\begin{aligned} \frac{\partial}{\partial \mu_L} \langle j_L(t) \rangle = & \frac{e}{\hbar} \left[\frac{4x^2}{\pi(1 + 2x^2)^2} + \sum_k J_k^2 \left(\frac{\Delta_d - \Delta_L}{\omega} \right) \right. \\ & F_1 \left(\frac{\Gamma^2(1 - 13x^2 + 4x^4)}{\pi(1 + 2x^2)^4} \right. \\ & \left. \left. + \frac{4\Gamma x(1 - 2x^2)}{\pi(1 + 2x^2)^3} F_2 \right) \right], \end{aligned} \quad (22)$$

where

$$F_1 = \left[\left(\mu_L - \varepsilon_d - \omega k + \frac{2\Gamma x}{1+2x^2} \right)^2 + \left(\frac{3\Gamma/2}{1+2x^2} \right)^2 \right]^{-1}, \quad (23)$$

$$F_2 = \left(\mu_L - \varepsilon_d - \omega k + \frac{2\Gamma x}{1+2x^2} \right). \quad (24)$$

Analyzing Eq. (22) one can find the origin of the asymmetric line shapes in differential conductance resulting from the interference of resonant and nonresonant tunneling paths. For the case of $V_{LR}=0$ we observe the Lorentzian resonances localized at $\varepsilon_d = \mu_L \pm \omega k$. The amplitudes of these resonances are determined by the k th-order Bessel functions calculated for the argument $(\Delta_d - \Delta_i)/\omega$. For the case of nonvanishing V_{LR} , the resulting curve is a superposition of the Lorentzian-like resonances and asymmetric parts weighed by the factors $\Gamma^2(1-13x^2+4x^4)/\pi(1+2x^2)^4$ and $4\Gamma x(1-2x^2)/\pi(1+2x^2)^3$, respectively. The Lorentzian-like resonance is centered at $\varepsilon_d = \mu_L \pm \omega k + 2\Gamma x/(1+2x^2)$ with the full width at half maximum (FWHM) equal to $3\Gamma/(1+2x^2)$ and the maximum value equal to $(4/9\pi)[(1-13x^2+4x^4)/(1+2x^2)^2]J_k^2[(\Delta_d - \Delta_L)/\omega]$. The asymmetric part of the differential conductance corresponding to the k th sideband is also centered in the same point with the distance between its maximum and minimum equal to $3\Gamma/(1+2x^2)$ and the absolute values of these extrema are equal to $(4/3\pi)[x(1-2x^2)/(1+2x^2)^2]J_k^2[(\Delta_d - \Delta_L)/\omega]$. For comparison, in the case of the QD coupled with two leads the corresponding Lorentzian-like part of the differential conductance corresponding to the k th sideband is centered at $\varepsilon_d = \mu_L \pm \omega k + \Gamma x/(1+x^2)$, with FWHM equal to $2\Gamma/(1+x^2)$ and the maximum value equal to $(1/2\pi)[(1-6x^2+x^4)/(1+2x^2)^2]J_k^2[(\Delta_d - \Delta_L)/\omega]$. Knowing the explicit expressions for the currents one can check the following relations between different elements of the conductance matrix $-e\partial\langle j_n(t)\rangle/\partial\mu_m$, e.g., Refs. 18 and 26. Current conservation implies $\sum_n \partial\langle j_n(t)\rangle/\partial\mu_m = 0$ where $n, m = L, R_1, R_2$. On the other hand, $\sum_m \partial\langle j_n(t)\rangle/\partial\mu_m = 0$ only for $\Delta_d - \Delta_L = \Delta_d - \Delta_{R_1} = \Delta_d - \Delta_{R_2}$. For other relations between the amplitudes Δ_d and $\Delta_L, \Delta_{R_1}, \Delta_{R_2}$ we have

$$\sum_k \partial\langle j_{R_1}(t)\rangle/\partial\mu_k = \sum_k \partial\langle j_{R_2}(t)\rangle/\partial\mu_k = -\frac{1}{2} \sum_k \partial\langle j_L(t)\rangle/\partial\mu_k \quad (25)$$

for $\Delta_d - \Delta_{R_1} = \Delta_d - \Delta_{R_2} \neq \Delta_d - \Delta_L$, and

$$\sum_k \partial\langle j_{R_1}(t)\rangle/\partial\mu_k \neq \sum_k \partial\langle j_{R_2}(t)\rangle/\partial\mu_k \neq \sum_k \partial\langle j_L(t)\rangle/\partial\mu_k \quad (26)$$

for $\Delta_d - \Delta_{R_1} \neq \Delta_d - \Delta_{R_2} \neq \Delta_d - \Delta_L$.

IV. RESULTS AND DISCUSSION

We consider the QD coupled with three, say the left, the first right, and the second right, metal leads with the additional overdot (bridge) couplings between the left and right

leads. First, in the Sec. IV A and IV B, we present the results for the time-averaged currents and derivatives of the average current with respect to the QD energy level in the presence of external microwave fields which are applied to the dot and three leads, respectively. Assuming the harmonic time modulation of the external fields, here we give the explicit formula for the averaged current, $\langle j_L(t)\rangle$, performing the corresponding integrals in the general formula given in Eq. (18), and compare it with the current $\langle j_L^{(2)}(t)\rangle$ flowing in the system of the QD coupled with two leads only (for the zero-temperature case):

$$\begin{aligned} \langle j_L(t)\rangle = & \frac{e}{\hbar} \sum_{i=R_1, R_2} \left\{ \frac{2x^2}{(1+2x^2)^2} (\mu_L - \mu_i) + \frac{\Gamma}{3\pi} \frac{1-13x^2+4x^4}{(1+2x^2)^3} \right. \\ & \times \sum_k \left[J_k^2 \left(\frac{\Delta_d - \Delta_L}{\omega} \right) \arctan(h_L^{(k)}) \right. \\ & \left. \left. - J_k^2 \left(\frac{\Delta_d - \Delta_i}{\omega} \right) \arctan(h_i^{(k)}) \right] \right. \\ & \left. + \frac{\Gamma x(1-2x^2)}{\pi(1+2x^2)^3} \sum_k \left[J_k^2 \left(\frac{\Delta_d - \Delta_L}{\omega} \right) \ln(g_L^{(k)}) \right. \right. \\ & \left. \left. - J_k^2 \left(\frac{\Delta_d - \Delta_i}{\omega} \right) \ln(g_i^{(k)}) \right] \right\}, \quad (27) \end{aligned}$$

where $h_i^{(k)} = [\mu_i - \varepsilon_d - \omega k + 2\Gamma x/(1+2x^2)]/[3\Gamma/2(1+2x^2)]$, $g_i^{(k)} = [\mu_i - \varepsilon_d - \omega k + 2\Gamma x/(1+2x^2)]^2 + [3\Gamma/2(1+2x^2)]^2$, and $i = L, R_1, R_2$, whereas for $\langle j_L^{(2)}(t)\rangle$ we have

$$\begin{aligned} \langle j_L^{(2)}(t)\rangle = & \frac{e}{\hbar} \left\{ \frac{2x^2}{\pi(1+x^2)^2} (\mu_L - \mu_R) + \frac{\Gamma}{2\pi} \frac{1-6x^2+x^4}{(1+2x^2)^3} \right. \\ & \times \sum_k \left[J_k^2 \left(\frac{\Delta_d - \Delta_L}{\omega} \right) \arctan(h_L^{(2k)}) \right. \\ & \left. \left. - J_k^2 \left(\frac{\Delta_d - \Delta_R}{\omega} \right) \arctan(h_R^{(2k)}) \right] \right. \\ & \left. + \frac{\Gamma x(1-x^2)}{\pi(1+x^2)^3} \sum_k \left[J_k^2 \left(\frac{\Delta_d - \Delta_L}{\omega} \right) \ln(g_L^{(2k)}) \right. \right. \\ & \left. \left. - J_k^2 \left(\frac{\Delta_d - \Delta_i}{\omega} \right) \ln(g_R^{(2k)}) \right] \right\}, \quad (28) \end{aligned}$$

where $h_i^{(2k)} = [\mu_i - \varepsilon_d - \omega k + \Gamma x/(1+2x^2)]/[\Gamma/(1+2x^2)]$ and $g_i^{(2k)} = [\mu_i - \varepsilon_d - \omega k + \Gamma x/(1+x^2)]^2 + \Gamma^2/(1+x^2)^2$, $i = L, R$. Note that $\langle j_L(t)\rangle$ consists of the two terms and each term is similar in its structure to the current flowing in the QD–two leads (QD–2l) system, $\langle j_L^{(2)}(t)\rangle$. However, due to the interference of the charge carriers propagating along the different ways, the arguments of the *inverse tangent* and *logarithmic* functions are different and the individual terms in $\langle j_L(t)\rangle$ and $\langle j_L^{(2)}(t)\rangle$ are weighted by different x -dependent factors. Second, in Sec. IV C, the time-dependent currents are also calculated in the case when the periodic or nonperiodic rectangular-pulse external fields are applied to each QD-lead barrier.

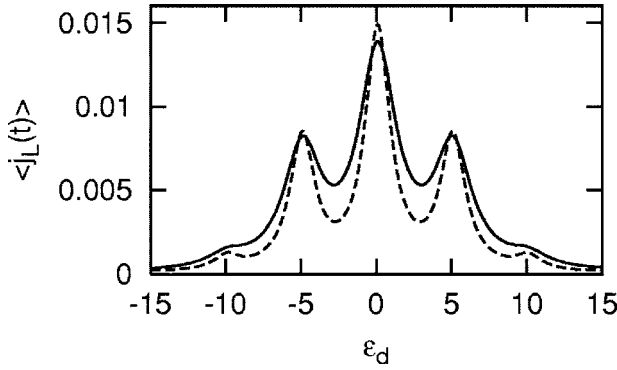


FIG. 2. The averaged current $\langle j_L(t) \rangle$ against the QD energy level ε_d in the system of a QD coupled with three (solid line) or two (broken line) leads. The microwave field is applied to the QD with the amplitude $\Delta_d=6$ and frequency $\omega=5$. The lead chemical potentials μ_L , μ_{R_1} , and μ_{R_2} are equal 0.2, 0.0, and 0.0, respectively, and the coupling between L and R_1 , R_2 leads is absent, $V_{LR}=0$. All energies are in Γ units and the current in $e\Gamma/\hbar$ units.

We have taken for V_{LR} the values comparable with $V_{\vec{k},\alpha d}$ and estimated $V_{\vec{k},\alpha d}$ (assuming its \vec{k} independence, $V_{\vec{k},\alpha d} \equiv V_\alpha = V$) using the relation $\Gamma_\alpha = 2\pi|V_\alpha|^2/D_\alpha$, where D_α is the α -lead bandwidth and $D_\alpha = 100\Gamma_\alpha$ ($\Gamma_L = \Gamma_R = \Gamma$, $D_L = D_R = D$ was assumed). We also assumed the zero-temperature case, as the temperature in the experiment is usually low. For calculations, we have chosen $e = \hbar = 1$ units and all energies are given in the Γ units.

A. Microwave field applied to the QD only

In Fig. 2 we compare the averaged values of the current flowing from the left lead in the systems in which the QD is coupled with three or two leads, the solid and broken curves, respectively. The external microwave field is applied only to the QD and dc bias between the left and right leads is small in comparison with ω , Δ_d , and Γ . The coupling V_{LR} is assumed to be zero. In such a case the sidebands on the current curve are clearly visible. The width of the corresponding peaks is smaller for the case of the QD coupled with two leads. Analyzing the expression for $\langle j_L(t) \rangle$ one can obtain (for $\mu_L \ll \Gamma$ and $\mu_{R_1} = \mu_{R_2} = 0$) the subsequent peaks in $\langle j_L(t) \rangle$ (as functions of ε_d) in the form $(4/9\pi)J_k^2(\Delta_d/\omega)\mu_L\{1 + [(\varepsilon_d + \omega k)/3\Gamma/2]^2\}^{-1}$ with the FWHM equal to 3Γ . For comparison, in the case of the QD coupled with two leads the corresponding peaks are described by the functions $(1/2\pi)J_k^2(\Delta_d/\omega)\mu_L\{1 + [(\varepsilon_d + \omega k)/\Gamma]^2\}^{-1}$ with the FWHM equal to 2Γ .

Next, we consider the case of a QD coupled with two leads with varying value of μ_R and compare it with the QD coupled with three leads (with the chemical potential of the third lead $\mu_{R_2} = -\mu_L$).

In Fig. 3 we present the results obtained for $\langle j_L(t) \rangle$ for the QD coupled with three (thick lines) or two (thin lines) leads. The upper (lower) panel corresponds to $x=0$ ($x=0.28$). For the case $\mu_L = -\mu_{R_1} = -\mu_{R_2} = 0.1$ and $x=0$ the sidebands are very clearly visible and the corresponding peaks are lower and broader for the QD–three leads (QD-3l) system as we

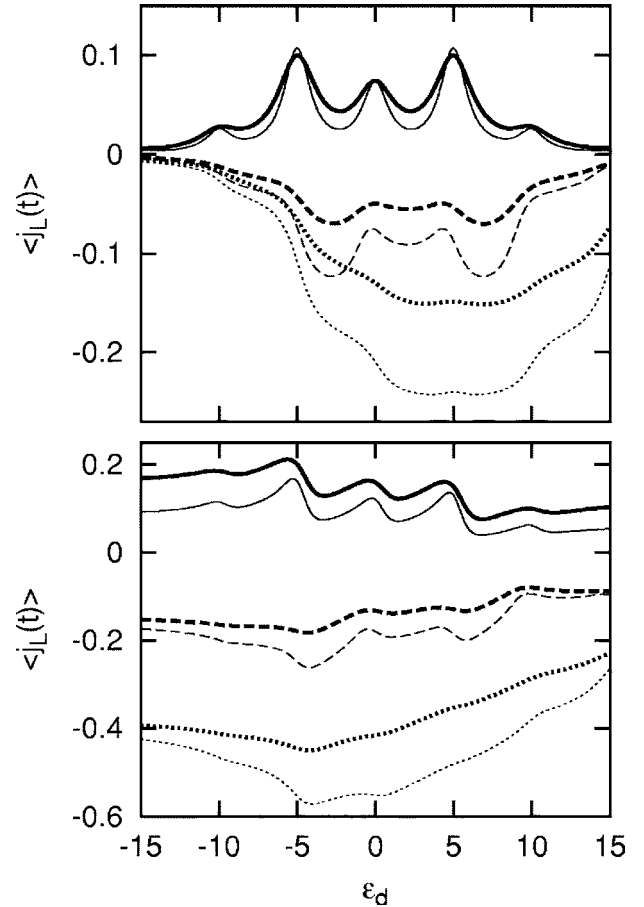


FIG. 3. The averaged current $\langle j_L(t) \rangle$ against ε_d in the system of a QD coupled with three (thick lines) or two (thin lines) leads. The upper (lower) panel corresponds to $x=0$ ($x=0.28$), x being the measure of the coupling between leads, $x = \pi V_{LR}/D$. In a QD–three leads system $\mu_L=0.1$, $\mu_{R_2}=-0.1$, and $\mu_{R_1}=-0.1$, 4, and 10 (solid, broken, and dotted curves, respectively). In a QD coupled with two leads $\mu_L=0.1$, $\mu_R=-0.1$, 4, and 10 (solid, broken, and dotted curves, respectively). $\omega=5$, $\Delta_d=8$, $\Delta_{R_1}=\Delta_{R_2}=\Delta_L=0$. The values of solid curves have been multiplied by a factor of 10 for the illustrating purposes.

discussed before (the upper panel, the solid lines). For the nonzero overdot coupling between the left and right leads the sideband peaks get asymmetric forms and for $x=0.28$ they become fully asymmetric (lower panel, solid lines). The current for the QD-2l system is also composed of a number of asymmetric components (thin solid lines) although now these forms are fully asymmetric for $x=0.41$ as we know from the earlier discussion. For greater values of μ_{R_1} , the corresponding current flowing in the QD-2l system achieves (for vanishing, as well as for nonzero coupling between leads) greater negative values and its dependence on the QD energy-level position is well marked in comparison to the results characterizing the QD-3l system.

Next, in Fig. 4 we analyze the influence of the overdot coupling between the left and right leads for broad range of this coupling. The thin (thick) lines correspond to the QD coupled with two (three) leads. We show $\langle j_L(t) \rangle$ for three values of the interleads coupling strength represented by the

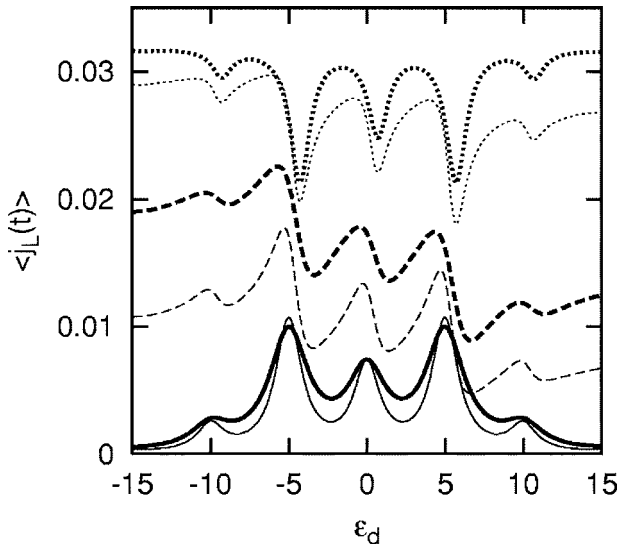


FIG. 4. The averaged current $\langle j_L(t) \rangle$ against ε_d in the system of a QD coupled with three (thick lines) or two (thin lines) leads. The solid, broken, and dotted curves correspond to $x=0$, 0.28, and 0.7, respectively. $\Delta_d=8$, $\Delta_{R_1}=\Delta_{R_2}=\Delta_L=0$, $\mu_L=-\mu_{R_1}=-\mu_{R_2}=0.1$, $\omega=5$.

parameter $x=\pi V_{LR}/D$. For $x=0$ we have well defined sideband peaks as previously shown in Fig. 2. Next, we show the results for $x=\sqrt{(13-\sqrt{153})/8}\approx 0.28$ and $x=\sqrt{2}/2\approx 0.7$. Note that the expression for $\langle j_L(t) \rangle$ [and $\langle j_L^{(2)}(t) \rangle$] consists of three terms. The first term depends on the difference $\mu_L-\mu_i$ and does not depend on the QD energy level ε_d . The second term corresponds to the Lorentzian-type contribution to a given sideband (it disappears for $x\approx 0.28$) and the last term corresponds to an asymmetric contribution (it disappears for $x\approx 0.7$), respectively. This last term influences the sideband shape only for nonvanishing overdot coupling between leads and is the most prominent sign of the interference effects. For $x=\sqrt{2}/2$ this term disappears and the resulting sidebands have a form of symmetric dips due to the negative value of the coefficient $\Gamma(1-13x^2+x^4)/[3\pi(1+2x^2)^3]$ in Eq. (27). In this case the nonresonant tunneling channels modify the dip's center position and its FWHM in comparison with the position and FWHM of sidebands presented for $x=0$. Note that for a QD coupled with two leads, the corresponding sidebands (the thin dotted line) are not fully symmetric curves as in this case the last term of Eq. (28) disappears for $x=1$ and not for $x=0.7$ (cf. Ref. 29). For $x\approx 0.28$ the corresponding sidebands are fully asymmetric curves as in this case the second term in Eq. (27) (which introduces asymmetry) disappears. Again, for a QD coupled with two leads the corresponding sidebands (the thin broken curve) are described by not fully asymmetric curves as the second term of Eq. (28), which gives a symmetric contribution to sidebands, disappears for $x=\sqrt{3-2\sqrt{2}}\approx 0.41$ and not for $x=0.28$.

In order to emphasize the influence of the additional lead on the currents and find the possible interference effects, we show in Fig. 5 the current $\langle j_L(t) \rangle$ for QD-2l and QD-3l systems calculated for the parameters for which the correspond-

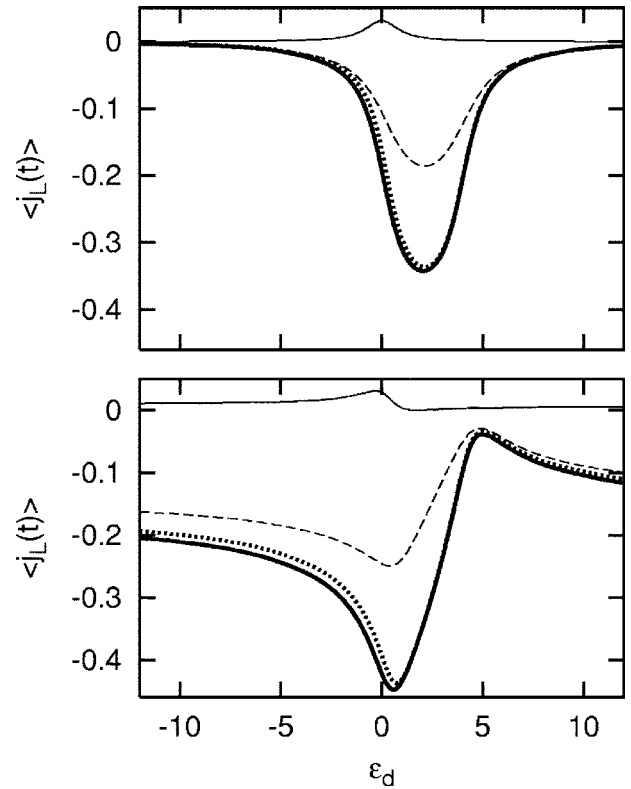


FIG. 5. The averaged current $\langle j_L(t) \rangle$ against ε_d for the QD-2l systems: $\mu_L=-\mu_R=0.1$ —thin solid lines and $\mu_L=0.1, \mu_R=4$ —thick solid lines and the QD-3l system: $\mu_L=-\mu_{R_1}=0.1, \mu_{R_2}=4$ —broken lines. The upper (lower) part corresponds to $x=0$ ($x=0.28$) and $\omega=5$, $\Delta_d=1$, $\Delta_{R_1}=\Delta_{R_2}=\Delta_L=0$. The dotted lines correspond to the sum of the currents flowing in two QD-2l systems.

ing curves are relatively simple. We assumed the small amplitude of the QD energy level oscillations, $\Delta_d=1$, and $\omega=5$, for which (for $x=0$) only the central peak corresponding to elastic tunneling is visible on the $\langle j_L(t) \rangle$ curves. We show $\langle j_L(t) \rangle$ obtained for two different QD-2l systems which can be viewed as components of the considered more complicated QD-3l system. We observe that due to the interference effects, the current $\langle j_L(t) \rangle$ flowing in the QD-3l system (the broken lines) is not simply a sum of currents (dotted lines) flowing in the corresponding QD-2l systems. The difference between this sum and the current corresponding to the QD-3l system is relatively large and exists independently of the coupling between leads.

In the next Fig. 6 we show all currents, $\langle j_L(t) \rangle$, $\langle j_{R_1}(t) \rangle$, and $\langle j_{R_2}(t) \rangle$, flowing in the QD-3l system for $x=0$ and $x=0.28$. For vanishing values of the overdot coupling the current $\langle j_L(t) \rangle$ is characterized by a sequence of the symmetric peaks, but the current $\langle j_{R_2}(t) \rangle$ is a superposition of the asymmetric structures placed in the points where the symmetric sidebands occur on $\langle j_L(t) \rangle$ curve. Analyzing the current $\langle j_{R_2}(t) \rangle$ according to Eq. (21) we have for the parameters in Fig. 6.

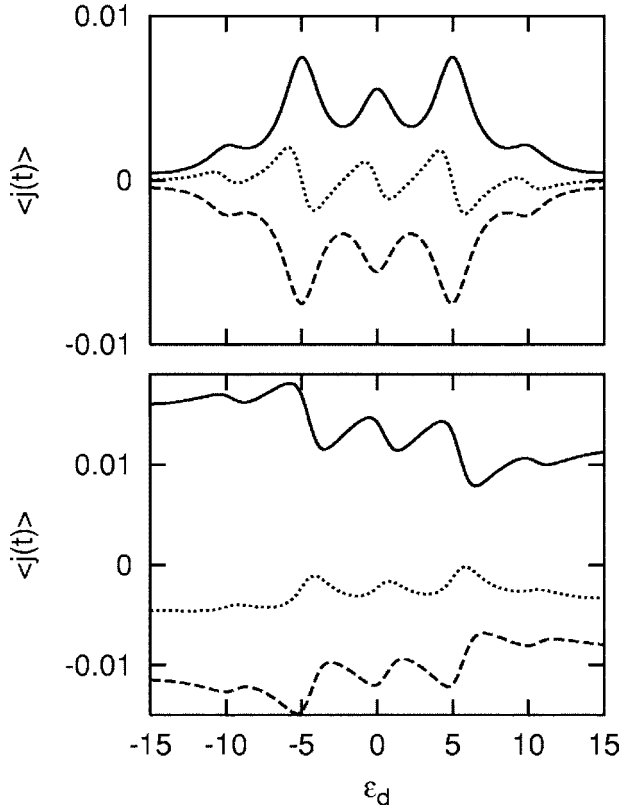


FIG. 6. The averaged currents $\langle j_L(t) \rangle$, $\langle j_{R_1}(t) \rangle$, and $\langle j_{R_2}(t) \rangle$ (solid, broken, and dotted lines, respectively) against ε_d in the system of a QD coupled with three leads. The upper (lower) panel corresponds to $x=0$ ($x=0.28$). $\Delta_d=8$ and other parameters are as in Fig. 4. The values of $\langle j_{R_2}(t) \rangle$ for $x=0$ (upper panel) have been multiplied by a factor of 20 for illustrating purposes.

$$\langle j_{R_2}(t) \rangle = \frac{e}{\hbar} \left[\frac{\Gamma}{3\pi} \sum_k J_k^2 \left(\frac{\Delta_d}{\omega} \right) [\arctan(h_{R_2}^{(k)}) - \arctan(h_L^{(k)}) + \arctan(h_{R_2}^{(k)}) - \arctan(h_{R_1}^{(k)})] \right], \quad (29)$$

where $h_i^{(k)} = (\mu_i - \varepsilon_d - \omega k) / (3\Gamma/2)$. One can see that each sideband is the sum of the peak [two first terms in Eq. (29)] and the dip [the last two terms in Eq. (29)] resulting in the asymmetric structure shown in Fig. 6

To learn more about the influence of the third electrode and additional overdot coupling between leads we present in Fig. 7 the currents $\langle j_L(t) \rangle$ for $x=0$ and $x=0.28$ and $\langle j_{R_2}(t) \rangle$ for $x=0$ as functions of the QD level position ε_d and the frequency ω of the microwave field applied to the QD. For vanishing coupling between leads ($x=0$) the current $\langle j_L(t) \rangle$ exhibits a well-known sideband structure for $\omega > \Gamma$ and for small frequencies, $\omega < \Gamma$, the two broad maxima at $\varepsilon_d = \pm \Delta_d$ are present. At the same time, the current $\langle j_{R_2}(t) \rangle$ exhibits the asymmetric structures centered on the (ε_d, ω) plane at the points where photon sidebands occur on the $\langle j_L(t) \rangle$ curves. These asymmetric structures on the $\langle j_{R_2}(t) \rangle$ curve exist also at $\omega < \Gamma$. On the other hand, a similar structure of the $\langle j_L(t) \rangle$ (the lower panel of Fig. 7) is obtained for $x=0.28$, i.e.,

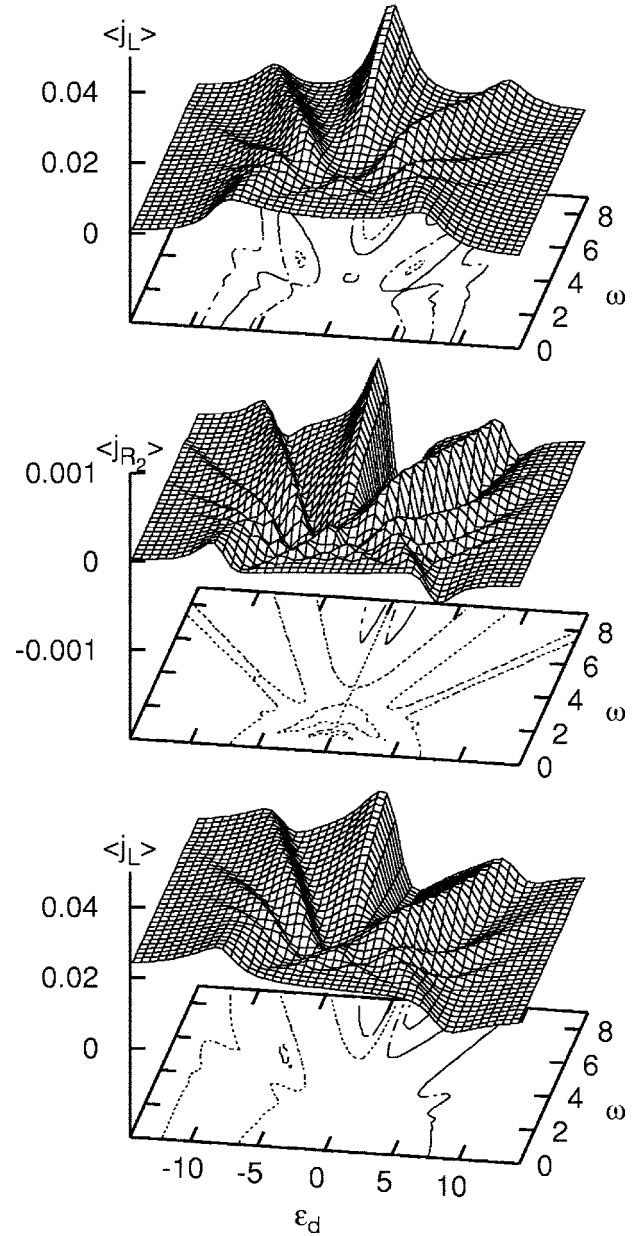


FIG. 7. The averaged currents against ε_d and ω . The upper (middle) panel shows $\langle j_L(t) \rangle \langle j_{R_2}(t) \rangle$ for $x=0$ and the lower panel gives $\langle j_L(t) \rangle$ for $x=0.28$. $\Delta_d=8$, $\Delta_{R_1}=\Delta_{R_2}=\Delta_L=0$, $\mu_L=-\mu_{R_1}=-\mu_{R_2}=0.2$.

we observe a number of asymmetric resonances separated by the photon energy for $\omega > \Gamma$. Notice the similarity of both pictures, i.e., $\langle j_L(t) \rangle$ calculated for $x=0.28$ and $\langle j_{R_2}(t) \rangle$ for $x=0$, respectively. Note, however, the different scale for these currents.

B. Microwave field applied to different parts of the system

In Fig. 8 we present $\langle j_L(t) \rangle$ for different overdot coupling assuming a strong asymmetry of the applied microwave field (ac potential is applied only to the R_1 lead in the QD-3I system). The additional R_2 lead is characterized by the chemical potential $\mu_{R_2} = (\mu_L + \mu_{R_1})/2 = 0$. For better demon-

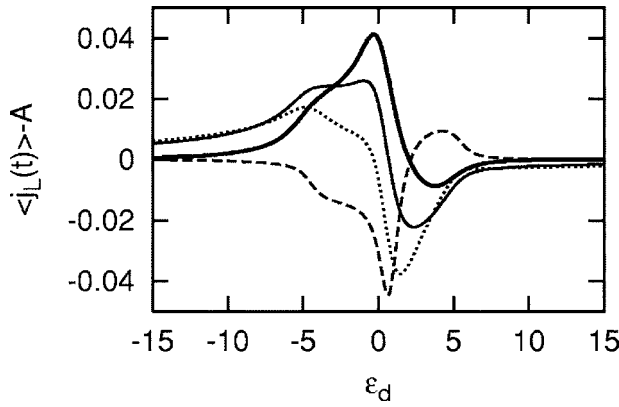


FIG. 8. The averaged current $\langle j_L(t) \rangle$ against ε_d for different values of the overdot coupling strength between the left and right leads. The thick solid, solid, dotted, and broken lines correspond to $x=0, 0.14, 0.28,$ and $0.7,$ respectively. $A=(e/\hbar)2x^2(2\mu_L-\mu_{R_1}-\mu_{R_2})/(1+2x^2)^2$ and $\Delta_{R_1}=3, \Delta_L=\Delta_{R_2}=\Delta_d=0, \mu_L=-\mu_{R_1}=0.2, \mu_{R_2}=0, \omega=5.$

stration of the influence of the ac potential on $\langle j_L(t) \rangle$ we moved down each curve by the constant value $A=(e/\hbar)2x^2(2\mu_L-\mu_{R_1}-\mu_{R_2})/(1+2x^2)^2$; see Eq. (27). This constant value does not depend on the ac field and is equal to the current obtained for the static case in the limit of large values of ε_d (the current between leads is practically induced by the overdot tunneling, only). For $x=0$ we observe a shoulder on the left side of the main peak and a small negative current for the positive values of ε_d . This picture is similar to the known results (for $x=0$) obtained experimentally and theoretically in the QD-2I systems, e.g., Refs. 3 and 35. With the increasing overdot coupling V_{LR} the height of the main resonant peak decreases and disappears for $x=0.28$. At the same time, for all values of x we observe a negative current for the small values of ε_d with a greater absolute value for stronger coupling between leads. For greater values of x the shape of the $\langle j_L(t) \rangle$ curve is changed dramatically and for $x=0.7,$ $\langle j_L(t) \rangle$ becomes nearly reversed in comparison with that calculated for $x=0$.

In Fig. 9 we analyze the influence of the third lead (here named as R_2) on the current $\langle j_L(t) \rangle$ when the external microwave field is applied to this lead and to the QD with $\Delta_d=2\Delta_{R_2}$. For comparison, we add in the upper panel the results for $\langle j_L(t) \rangle$ obtained for the case when this additional third lead is not irradiated by the microwave field. In this case, as before, see, e.g., Fig. 2, we observe typical sidebands on the current curves (the difference between the lead chemical potentials is small in comparison with the amplitude Δ_d). However, after including the third lead irradiated by the external microwave field the dependence of the current $\langle j_L(t) \rangle \equiv j_L$ on the gate voltage (or equivalently on the QD energy level position) is quite different—compare the thin or thick solid lines of the upper and lower panels. For smaller values of Δ_d and Δ_{R_2} , the averaged current j_L is very similar to the corresponding current J_L obtained by applying the external microwave field only to one lead (see the thick solid line in Fig. 8). These curves are, however, related between themselves by a relation $J_L(\varepsilon_d) \approx j_L(-\varepsilon_d)$. Now we can observe a small nega-

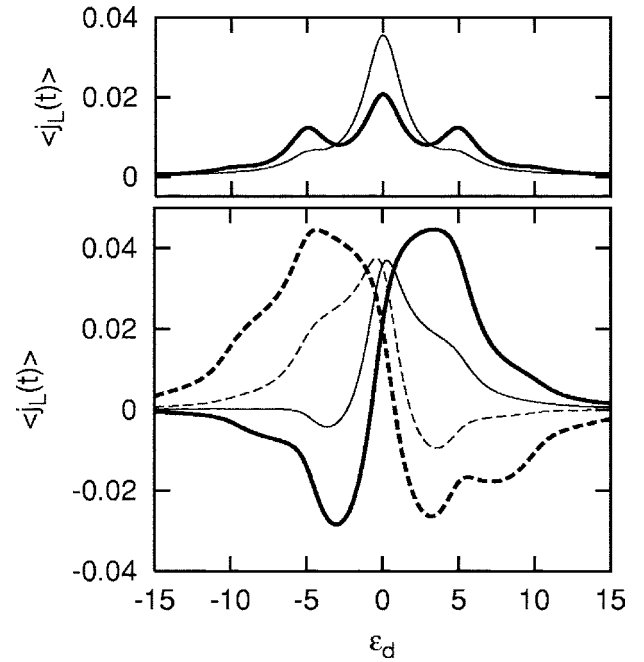


FIG. 9. The averaged current $\langle j_L(t) \rangle$ against ε_d for the case of the microwave field applied only to the QD with $\Delta_d=3$ (thin line) or $\Delta_d=6$ (thick line)—upper panel. The lower panel corresponds to the case of the microwave field applied to the QD and R_2 lead with $\Delta_d=2\Delta_{R_2}$ and $\Delta_{R_2}=1.5$ or 3 (thin or thick lines, respectively). The broken lines show the results when the microwave field applied to the QD and R_2 lead are out of phase (with the phase difference of π), $\mu_L=-\mu_{R_1}=0.2, \mu_{R_2}=0, \omega=5.$

tive current at small negative values of ε_d and some enhancement of the current on the right side of the main peak. Similarly, the significant differences between the corresponding currents are observed also for greater values of the amplitudes Δ_d and Δ_{R_2} (compare the thick solid lines in the upper and lower panels of Fig. 9). Note that very similar behavior of the current $\langle j_L(t) \rangle$ as the function of the gate voltage is observed if we compare the case when the microwave field is applied only to one lead and the case when the microwave field is applied simultaneously to the QD and R_2 lead but with the phase difference of π —compare the thin broken curve in Fig. 9 with the thick solid curve in Fig. 8.

In order to present more information about the differences between the electron transport in the QD-3I and QD-2I systems we display in Fig. 10 the derivative $d\langle j_L(t) \rangle/d\varepsilon_d$ as a function of ε_d and ω . The lowest panel corresponds to the QD-3I system and two other panels correspond to the QD-2I systems. These QD-2I systems are characterized by such parameters that combined together give us the considered QD-3I system. One can see that the considered characteristics of the electron transport in the QD-3I system are not simply the algebraic sum of the corresponding curves of both QD-2I systems. In all three cases shown in Fig. 10, the position of the corresponding minima and maxima (along the ε_d axis) can be identified with the values of the leads chemical potentials. However, the corresponding structures are less clear in the case of the QD-3I system in comparison with those for the QD-2I models.

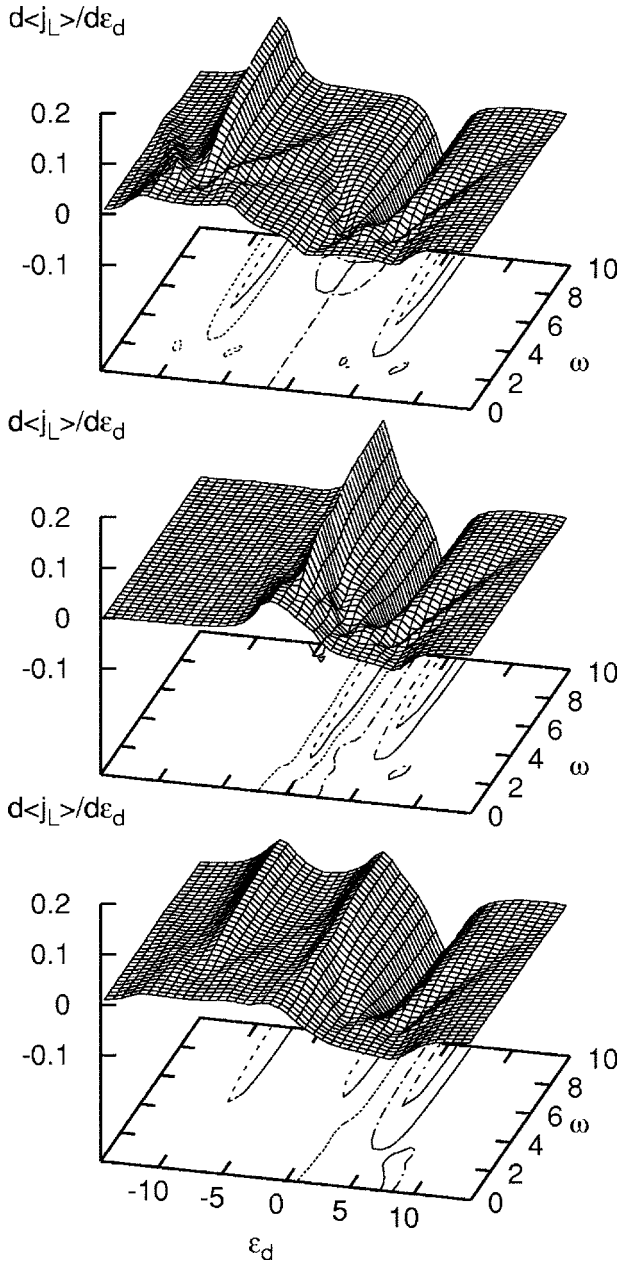


FIG. 10. The averaged current derivatives $d\langle j_L(t) \rangle / d\varepsilon_d$ against ε_d and ω for $x=0$. We compare the results obtained for the QD coupled with two leads—the upper (middle) panel—for $\mu_L=5$, $\mu_R=-8$, $\Delta_L=8$, $\Delta_d=4$, $\Delta_R=0$ ($\mu_L=5$, $\mu_R=0$, $\Delta_L=8$, $\Delta_d=4$, $\Delta_R=2$) with the results obtained for the QD coupled with three leads—the lower panel— $\Delta_L=8$, $\Delta_d=4$, $\Delta_{R_1}=2$, $\Delta_{R_2}=0$, $\mu_L=5$, $\mu_{R_1}=0$, $\mu_{R_2}=-8$, $\omega=5$.

C. Rectangular-pulse modulation of the couplings between QD and leads

In the next step of our investigations of the electron transport in the QD-3l systems we consider the time-dependent currents flowing in response to the time-dependent barriers between the QD and leads or in response to suddenly removed (or inserted) connection of the QD with one of the leads. First we assume a rectangular-pulse modulation applied to the QD- R_1 lead and QD- R_2 lead barriers. We assume

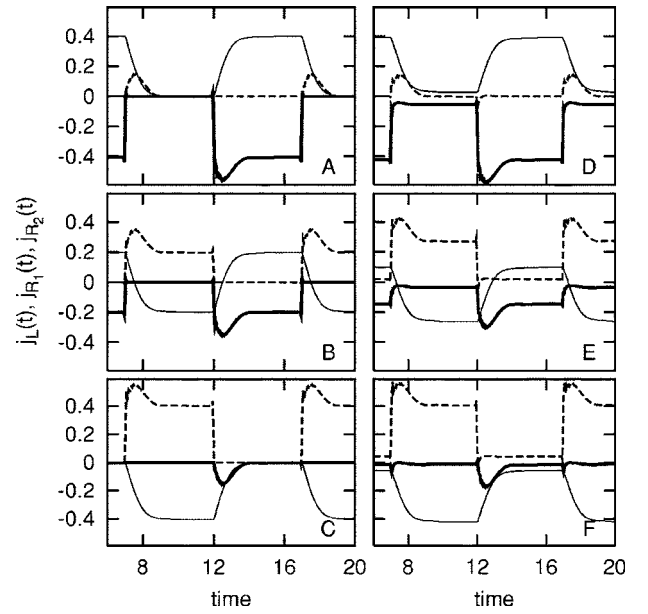


FIG. 11. The time-dependent current flowing in the system of a QD coupled with the three leads: L , R_1 , and R_2 . The L lead is coupled with the QD only—the left panels, and with the QD and two other leads, $V_{LR_1}=V_{LR_2}=4$ —the right panels. The couplings between the QD and R_1 , R_2 leads are changed periodically. The upper, middle, and lower panels correspond to $\mu_L=3$, 0 , and -3 , respectively. $-\mu_{R_1}=\mu_{R_2}=3$, $\varepsilon_d=0$. The thin, thick, and broken curves correspond to j_L , j_{R_1} , and j_{R_2} currents, respectively. The time is in \hbar/Γ units and currents are in $e\Gamma/\hbar$ units.

that these modulations are with a phase difference of π . In the first (second) half cycle, $V_{dR_1}=0$ ($V_{dR_2}=0$) and the QD is coupled only to the R_2 lead (R_1 lead). In addition, the QD is coupled to the next, say L lead, with a constant value V_{dL} . In the following we consider the time-dependent currents $j_L(t)$, $j_{R_1}(t)$, and $j_{R_2}(t)$ for the three specific conditions: $\mu_L=\mu_{R_2}$, $\mu_L=(\mu_{R_1}+\mu_{R_2})/2$, and $\mu_L=\mu_{R_1}$. In addition, we assume $\mu_{R_2}=-\mu_{R_1}=3$, $\varepsilon_d=\mu_{R_1}$, and take for the period of the considered barrier modulation $T=5$. In a such case we integrate numerically the corresponding set of the differential equations for the matrix elements of the evolution operator and in the next step calculate the currents according to the formula $j_a(t)=-e dn_a(t)/dt$, where $a=L, R_1$, or R_2 and $n_a(t)$ is given in Eq. (5) (or similar to it). We checked that the QD charge hardly depends on the additional V_{LR} couplings. Although the QD charge is almost insensitive to the additional overdot couplings the currents demonstrate such dependence. Especially visible are the differences for the case when the chemical potential μ_L of the third electrode L lies between the chemical potentials of two other leads; see Figs. 11(B) and 11(E). For other values of μ_L , the influence of the overdot tunneling channels for the parameters considered here is smaller. Note that after abrupt changing of the coupling between the QD and R_1 or R_2 leads the currents j_L , j_{R_1} , and j_{R_2} rapidly change too, and after a short time reach the steady values. The QD coupled with three leads could be considered as the three-state system. We observe that for some values of the lead chemical potentials the currents change their values periodically, e.g., from zero to the positive value [see j_{R_2} in

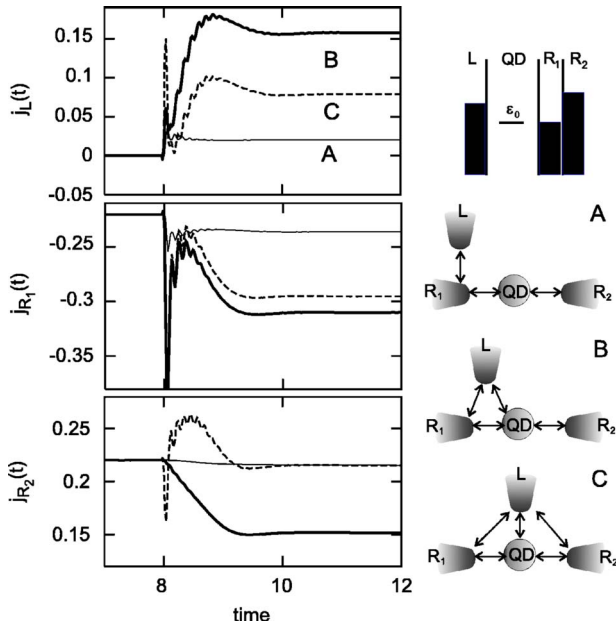


FIG. 12. (Color online) The time-dependent currents flowing from the L , R_1 , and R_2 leads in the system shown in Fig. 1. The thin solid, thick solid, and broken curves correspond to different couplings of the L lead to the other elements of the system: ($V_{LR_1}=4, V_{Ld}=V_{LR_2}=0$), ($V_{LR_1}=4, V_{Ld}=4, V_{LR_2}=0$), and ($V_{LR_1}=V_{Ld}=V_{LR_2}=4$), respectively.

Fig. 11(B)], from zero to the negative value [see j_{R_1} in Fig. 11(B)] or from the negative to the positive value [see j_L in Fig. 11(B)]. The additional couplings between leads modify the values of the currents but the qualitative picture remains the same. Note that in the first moment after abrupt changing of the coupling between the QD and R_1 or R_2 lead we have $j_L(t)+j_{R_1}(t)+j_{R_2}(t) \neq 0$ as in this case $dn_d(t)/dt \neq 0$ (not shown here). After some delay time the QD charge stabilizes around its equilibrium value, the currents tend to constant values and their sum is equal to zero.

In the last step we consider the response of the currents to the abrupt inclusion into the QD-2l system of the third electrode (in our case, L lead). The results are presented in Fig. 12 together with the schematic view of the subsequent tunnel connections between the QD and the three leads. We show the time-dependent currents $j_L(t)$, $j_{R_1}(t)$, and $j_{R_2}(t)$ corresponding to the three different ways of inclusion of the L lead. We assumed the chemical potentials $\mu_{R_1}=-\mu_{R_2}$, $\mu_L=(\mu_{R_1}+\mu_{R_2})/2$, and $\varepsilon_d=\mu_{R_1}$. Consider the current j_{R_2} flowing from the R_2 lead characterized by the highest chemical potential μ_{R_2} . Before adding to the system of the L lead (see case A in Fig. 12) the current j_{R_2} has a constant value and flows from the R_2 lead through the QD energy level to the R_1 lead. When the L lead is included into the system (the tunneling coupling V_{LR_1} changes abruptly at $t=8$ from the zero to nonzero value) the current j_{R_2} is almost unchanged—its value decreases slightly without any transients at short times after the time $t=8$ (thin solid line). Next, we consider the case when the L lead is abruptly connected simultaneously with the QD and R_1 lead (case B in Fig. 12). Now the current j_{R_2} (thick solid line) decreases significantly during the short

time after the moment of inclusion of the L lead and settles to its constant value. Note that j_{R_2} decreases despite the additional charge transfer channel between R_2 and L leads (through the QD energy level). The destructive interference appears in this case as we have two transmission channels for tunneling electrons between R_2 and R_1 leads. However, the constructive interference is visible if we consider the next case when the L lead is abruptly coupled with the QD-2l system assuming nonzero values of V_{LR_1} , V_{LR_2} , and V_{Ld} (broken line). Now, we have one additional charge-transfer channel (from the R_2 lead) in comparison with the former case. The current j_{R_2} rapidly increases with some fluctuations and after the time $\sim \hbar/\Gamma$ decreases to the constant value. A similar analysis can be made considering the currents j_L and j_{R_1} although the transient current changes are more visible now at short times after the abrupt inclusion of additional electron tunneling channels. The above discussion concerns the specific values of the lead chemical potentials and the position of the QD energy level. Nevertheless, similar qualitative conclusions can be made also for other values characterizing the considered system.

V. CONCLUSIONS

We have studied the time-dependent tunneling transport through the QD coupled with three metal leads using the evolution operator technique. The time-dependent QD charge and currents were determined in terms of the appropriate evolution operator matrix elements. Applying the wide-band limit to the integrodifferential equations satisfied by the evolution operator matrix elements we were able to give the analytical expressions for the time-averaged currents and differential conductance. We considered the external harmonic microwave fields applied to different parts of the considered system, as well as the rectangular-pulse modulation imposed on different QD-lead barriers. In addition, we have studied also the time dependence of the currents due to abrupt inclusion into the QD–two leads system of the third electrode. We have considered also the effect of the additional couplings between leads (we coupled one of the leads with the other two leads) on the conductance and current flowing in the system. Our main results can be summarized as follows:

(i) For the vanishing nonresonant tunneling path, $V_{LR}=0$, and for the parameters for which the photon-assisted sidebands are clearly visible on the $\langle j_L(t) \rangle$ curve the subsequent sideband peaks have the Lorentz-type form with the FWHM equal to 3Γ in comparison with 2Γ for the QD–two leads system. For the increasing value of V_{LR} the form of the sidebands transforms from the Lorentz type to the fully asymmetric form for $x=\sqrt{(13-\sqrt{153})}/8 \approx 0.28$. For greater x the form of the sidebands changes and gains again the Lorentz-type shape for $x=\sqrt{2}/2$. For the QD coupled with two leads the corresponding values of x are equal to $\sqrt{3-2\sqrt{2}} \approx 0.41$ and 1, respectively.

(ii) For the vanishing V_{LR} the differential conductance curve, e.g., $d\langle j_L(t) \rangle/d\mu_L$, possesses the sidebands of the Lorentz type localized at $\mu_L=\varepsilon_d \pm \omega k$. For $V_{LR} \neq 0$ these sidebands are described by the superposition of two parts, the

Lorentz-type and the asymmetric one centered at $\varepsilon_d = \mu_L \pm \omega k + 2\Gamma x / (1 + 2x^2)$ weighed by the factors $[\Gamma(1 - 13x^2 + 4x^4) / \pi(1 + 2x^2)^4] J_k^2[(\Delta_d - \Delta_L) / \omega]$ and $[4\Gamma x(1 - 2x^2) / (1 + 2x^2)^3] J_k^2[(\Delta_d - \Delta_L) / \omega]$, respectively. For the QD–two leads system the corresponding k th sidebands are centered at $\varepsilon_d = \mu_L \pm \omega k + \Gamma x / (1 + x^2)$ and their symmetric and asymmetric parts are weighed by the factors $[\Gamma^2(1 - 6x^2 + x^4) / \pi(1 + x^2)^4] J_k^2[(\Delta_d - \Delta_L) / \omega]$ and $[2\Gamma x(1 - x^2) / \pi(1 + x^2)^3] J_k^2[(\Delta_d - \Delta_L) / \omega]$, respectively.

(iii) The symmetry properties of the sidebands corresponding to the current flowing from the given lead depend on the position of the chemical potential of this lead in comparison with the chemical potentials of the other two leads. Taking, for example, $V_{LR} = 0$ and μ_{R_2} localized in the middle between μ_L and μ_{R_1} one can observe on the $\langle j_L(t) \rangle$ curve the sidebands of nearly regular (Lorentz-type) forms while the sidebands on the $\langle j_{R_2}(t) \rangle$ curve have asymmetric structures. However, in the presence of the nonresonant tunneling path the sidebands on the $\langle j_L(t) \rangle$ curve change their form and for $x \approx 0.28$ they have a fully asymmetric shape. On the other hand, the sidebands on the $\langle j_{R_2}(t) \rangle$ curve have for $x \approx 0.28$ a nearly Lorentz-like shape.

(iv) Especially large interference effects can be observed if we compare the current flowing in the QD-3l system with the sum of currents flowing in the two QD-2l systems which can be viewed as the components of the considered more complicated QD-3l system. The difference between them is relatively large independently of the overdot coupling between leads (see Fig. 5).

(v) In the case of strong asymmetry of the applied external field ($\Delta_{R_1} \neq 0, \Delta_L = \Delta_d = \Delta_{R_2} = 0$) we observe for $x = 0$ a shoulder on the left side of the main resonant peak on the $\langle j_L(t) \rangle$ curve vs the gate voltage. With the increasing overdot coupling between L and R_1, R_2 leads the main resonant peak disappears and transforms in a dip for strong coupling V_{LR} .

(vi) Let us consider the time dependence of currents flowing in response to the time-dependent barriers between the QD and two leads (we assume a constant coupling of the QD with the third lead). For the assumed rectangular-pulse modulation applied to the QD– R_1 and QD– R_2 lead barriers one can consider the QD-3l system as a three-state one. For example, the currents $j_L(t)$, $j_{R_1}(t)$, and $j_{R_2}(t)$ change their values periodically between zero and positive, positive and zero, and negative and positive values, respectively [see Fig. 11(B)]. The additional couplings between the leads introduce only small quantitative changes.

ACKNOWLEDGMENTS

The work of T.K. has been supported by the Foundation for Polish Science and the work of R.T. has been partially supported by KBN Grant No. PBZ-MIN-008/P03/2003.

APPENDIX

In this section we present the derivations of the general equations satisfied by the required functions $U_{dd}(t, t_0)$, $U_{\vec{k}d}(t, t_0)$, $U_{d, \vec{\eta}\vec{q}}(t, t_0)$ and $U_{\vec{k}d}(t, t_0)$, $U_{\vec{k}_1, \vec{k}_2}(t, t_0)$, $U_{\vec{k}, \vec{\eta}\vec{q}}(t, t_0)$

needed for the calculations of the QD charge $n_d(t)$ and the currents flowing in the considered system. In the next step, using the WBL approximation we simplify these equations and give the analytical solutions for them. Let us begin from the derivation of the integrodifferential equation satisfied by $U_{dd}(t, t_0)$. Writing down the formal solution of Eq. (9),

$$U_{\vec{q}\vec{r}d}(t, t_0) = -i \int_{t_0}^t dt_1 \tilde{V}_{\vec{q}\vec{r}d}(t_1) U_{dd}(t_1, t_0) - i \int_{t_0}^t dt_1 \sum_{\vec{k}} \tilde{V}_{\vec{q}\vec{r}\vec{k}}(t_1) U_{\vec{k}d}(t_1, t_0) \quad (\text{A1})$$

and inserting them to the formal solution of Eq. (8),

$$U_{\vec{k}d}(t, t_0) = -i \int_{t_0}^t dt_1 \tilde{V}_{\vec{k}d}(t_1) U_{dd}(t_1, t_0) - i \int_{t_0}^t dt_1 \sum_{\vec{p}=\vec{q}, \vec{r}} \tilde{V}_{\vec{k}\vec{p}}(t_1) U_{\vec{p}d}(t_1, t_0), \quad (\text{A2})$$

one can obtain after straightforward calculations the function $U_{\vec{k}d}(t, t_0)$ expressed in the terms of $U_{dd}(t, t_0)$, only,

$$U_{\vec{k}d}(t, t_0) = (-i) \int_{t_0}^t dt_1 \tilde{V}_{\vec{k}d}(t_1) U_{dd}(t_1, t_0) + (-i)^2 \int_{t_0}^t \int_{t_0}^{t_1} dt_1 dt_2 R_{\vec{k}d}(t_1, t_2) U_{dd}(t_2, t_0) + \sum_{j=2}^{\infty} (-i)^{2j} \int_{t_0}^t \int_{t_0}^{t_1} \cdots \int_{t_0}^{t_{2j-1}} dt_1 \cdots dt_{2j} \times \sum_{\vec{k}_1, \vec{k}_2, \dots, \vec{k}_{j-1}} R_{\vec{k}\vec{k}_1}^{\vec{z}}(t_1, t_2) R_{\vec{k}_2\vec{k}_3}^{\vec{z}}(t_3, t_4) \cdots R_{\vec{k}_{j-1}d}^{\vec{z}}(t_{j-1}, t_j) U_{dd}(t_j, t_0) + \sum_{j=1}^{\infty} (-i)^{2j+1} \int_{t_0}^t \int_{t_0}^{t_1} \cdots \int_{t_0}^{t_{2j}} dt_1 \cdots dt_{2j+1} \times \sum_{\vec{k}_1, \vec{k}_2, \dots, \vec{k}_j} R_{\vec{k}\vec{k}_1}^{\vec{z}}(t_1, t_2) R_{\vec{k}_2\vec{k}_3}^{\vec{z}}(t_3, t_4) \cdots \tilde{V}_{\vec{k}, d}^{\vec{z}}(t_{2j+1}) U_{dd}(t_{2j+1}, t_0), \quad (\text{A3})$$

where

$$R_{ij}(t_1, t_2) = \sum_{\vec{q}} \tilde{V}_{i\vec{q}}(t_1) \tilde{V}_{\vec{q}j}(t_2) + \sum_{\vec{r}} \tilde{V}_{i\vec{r}}(t_1) \tilde{V}_{\vec{r}j}(t_2). \quad (\text{A4})$$

We remember that the wave vectors \vec{k} , \vec{q} , and \vec{r} correspond to the left lead and the first and second right leads, respectively. Inserting into Eq. (7) the expressions for the functions $U_{\vec{q}d}(t, t_0)$, $U_{\vec{r}d}(t, t_0)$, and $U_{\vec{k}d}(t, t_0)$, Eqs. (A1)–(A3), we can write the integrodifferential equation for $U_{dd}(t, t_0)$ in the form

$$\begin{aligned}
\frac{\partial U_{dd}(t, t_0)}{\partial t} = & - \int_{t_0}^t dt_1 \left[\sum_{\bar{k}} \tilde{V}_{d\bar{k}}(t) \tilde{V}_{\bar{k}d}(t_1) + R_{dd}(t, t_0) \right] U_{dd}(t_1, t_0) \\
& + \sum_{j=1}^{\infty} (-i)^{2j-1} \int_{t_0}^t \int_{t_0}^{t_1} \cdots \int_{t_0}^{t_{2j-1}} dt_1 \cdots dt_{2j} \sum_{\bar{k}_1, \bar{k}_2, \dots, \bar{k}_j} [R_{d\bar{k}_1}(t, t_1) R_{\bar{k}_1 \bar{k}_2}(t_2, t_3) \cdots \\
& R_{\bar{k}_{j-1} \bar{k}_j}(t_{2j-2}, t_{2j-1}) \tilde{V}_{\bar{k}_j d}(t_2j) \\
& + \tilde{V}_{d\bar{k}_1}(t) R_{\bar{k}_1 \bar{k}_2}(t_1, t_2) \cdots R_{\bar{k}_j d}(t_{2j-1}, t_{2j})] U_{dd}(t_{2j}, t_0) \\
& + \sum_{j=1}^{\infty} (-i)^{2j} \int_{t_0}^t \int_{t_0}^{t_1} \cdots \int_{t_0}^{t_{2j}} dt_1 \cdots dt_{2j+1} \sum_{\bar{k}_1 \bar{k}_2 \dots \bar{k}_j} [R_{d\bar{k}_1}(t, t_1) R_{\bar{k}_1 \bar{k}_2}(t_2, t_3) \cdots \\
& R_{\bar{k}_{j-1} \bar{k}_j}(t_{2j-2}, t_{2j-1}) R_{\bar{k}_j d}(t_{2j}, t_{2j+1}) \\
& + \sum_{\bar{k}_{j+1}} \tilde{V}_{d\bar{k}_1}(t) R_{\bar{k}_1 \bar{k}_2}(t_1, t_2) \cdots R_{\bar{k}_j \bar{k}_{j+1}}(t_{2j-1}, t_{2j}) \tilde{V}_{\bar{k}_{j+1} d}(t_{2j+1})] U_{dd}(t_{2j+1}, t_0). \tag{A5}
\end{aligned}$$

This rather untractable general equation can be greatly simplified using the WBL approximation. Assuming $V_{d\bar{r}} = V_{d\bar{q}} = V_{d\bar{k}} \equiv V$, $V_{\bar{r}\bar{k}} = V_{\bar{q}\bar{k}} \equiv V_{LR}$, the multidimensional time integrations and summations over the wave vectors can be performed giving in result Eq. (12) with the solution

$$U_{dd}(t, t_0) = \exp[-C_1(t - t_0)]. \tag{A6}$$

Here $C_1 = \frac{3}{2}\Gamma - \Gamma[(3x^2 + 2ix)/(1 + 2x^2)]$ and $x = \pi V_{RL}/D$, D being the bandwidth of the lead energy band ($D_{R_1} = D_{R_2} = D_L = D$). The function $U_{\bar{k}d}(t, t_0)$ given in Eq. (A3) can be reduced within the WBL approximation to the form

$$U_{\bar{k}d}(t, t_0) = -C_2 \int_{t_0}^t dt_1 \tilde{V}_{\bar{k}d}(t_1) U_{dd}(t_1, t_0), \tag{A7}$$

where

$$C_2 = \frac{i + 2x}{1 + 2x^2}. \tag{A8}$$

In order to calculate $U_{d\bar{k}}(t, t_0)$ we write down accordingly with Eq. (3) the corresponding set of coupled differential equations for the functions $U_{d\bar{k}}(t, t_0)$, $U_{\bar{k}_1 \bar{k}_2}(t, t_0)$, $U_{\bar{q}\bar{r}}(t, t_0)$,

and $U_{\bar{r}\bar{k}}(t, t_0)$. The subsequent steps of the calculations are similar to those performed in the derivation of Eq. (A5). Inserting the formal solutions for $U_{\bar{k}_1 \bar{k}_2}(t, t_0)$, $U_{\bar{q}\bar{r}}(t, t_0)$,

$$\begin{aligned}
U_{\bar{k}_1 \bar{k}_2}(t, t_0) = & \delta_{\bar{k}_1 \bar{k}_2} - i \int_{t_0}^t dt_1 \left[\tilde{V}_{\bar{k}_1 d}(t_1) U_{d\bar{k}_2}(t_1, t_0) \right. \\
& \left. + \sum_{\bar{p}=\bar{q}\bar{r}} \tilde{V}_{\bar{k}_1 \bar{p}}(t_1) U_{\bar{p}\bar{k}_2}(t_1, t_0) \right], \tag{A9}
\end{aligned}$$

$$\begin{aligned}
U_{\bar{p}\bar{k}}(t, t_0) = & -i \int_{t_0}^t dt_1 \left[\tilde{V}_{\bar{p}d}(t_1) U_{d\bar{k}}(t_1, t_0) \right. \\
& \left. + \sum_{\bar{k}_1} \tilde{V}_{\bar{p}\bar{k}_1}(t_1) U_{\bar{k}_1 \bar{k}}(t_1, t_0) \right], \tag{A10}
\end{aligned}$$

into the differential equation satisfied by $U_{d\bar{k}}(t, t_0)$ one obtains the derivative $\partial U_{d\bar{k}}(t, t_0)/\partial t$ expressed in terms of $U_{d\bar{k}}(t, t_0)$ and $U_{\bar{k}_1 \bar{k}_2}(t, t_0)$. On the other hand, on the basis of Eqs. (A9) and (A10) the function $U_{\bar{k}_1 \bar{k}_2}(t, t_0)$ can be represented in the form containing only $U_{d\bar{k}}(t, t_0)$. Finally, one obtains

$$\begin{aligned}
\frac{\partial U_{d\bar{k}}(t, t_0)}{\partial t} = & -i \tilde{V}_{d\bar{k}}(t) + (-i)^2 \int_{t_0}^t dt_1 \left[\sum_{\bar{q}_1} \tilde{V}_{d\bar{q}_1} \tilde{V}_{\bar{q}_1 \bar{k}}(t_1) + \sum_{\bar{r}_1} \tilde{V}_{d\bar{r}_1}(t) \tilde{V}_{\bar{r}_1 \bar{k}}(t_1) \right] \\
& + (-i)^3 \int_{t_0}^t \int_{t_0}^{t_1} dt_1 dt_2 \left[\sum_{\bar{k}_1, \bar{q}_1} \tilde{V}_{d\bar{k}_1}(t) \tilde{V}_{\bar{k}_1 \bar{q}_1}(t_1) \tilde{V}_{\bar{q}_1 \bar{k}}(t_2) + \sum_{\bar{k}_1, \bar{r}_1} \cdots \right] \\
& + (-i)^4 \int_{t_0}^t \int_{t_0}^{t_1} \int_{t_0}^{t_2} dt_1 dt_2 dt_3 \left[\sum_{\bar{q}_1, \bar{k}_1, \bar{q}_2} \tilde{V}_{d\bar{q}_1}(t) \tilde{V}_{\bar{q}_1 \bar{k}_1}(t_1) \tilde{V}_{\bar{k}_1 \bar{q}_2}(t_2) \tilde{V}_{\bar{q}_2 \bar{k}}(t_3) + \sum_{\bar{r}_1, \bar{k}_1, \bar{q}_2} \cdots + \sum_{\bar{q}_1 \bar{k}_1 \bar{r}_2} \cdots + \sum_{\bar{r}_1 \bar{k}_1 \bar{r}_2} \cdots \right] + \cdots \\
& + (-i)^2 \int_{t_0}^t dt_1 \left[\sum_{\bar{k}_1} \tilde{V}_{d\bar{k}_1}(t) \tilde{V}_{\bar{k}_1 d}(t_1) + \sum_{\bar{q}_1} \tilde{V}_{d\bar{q}_1}(t) \tilde{V}_{\bar{q}_1 d}(t_1) + \sum_{\bar{r}_1} \tilde{V}_{d\bar{r}_1}(t) \tilde{V}_{\bar{r}_1 d}(t_1) \right] U_{d\bar{k}}(t_1, t_0)
\end{aligned}$$

$$+ (-i)^3 \int_{t_0}^t \int_{t_0}^{t_1} dt_1 dt_2 \left[\sum_{\vec{k}_1, \vec{q}_1} \tilde{V}_{d\vec{k}_1}(t) \tilde{V}_{\vec{k}_1 \vec{q}_1}(t_1) \tilde{V}_{\vec{q}_1 d}(t_2) + \sum_{\vec{k}_1, \vec{r}_1} \cdots + \sum_{\vec{q}_1 \vec{k}_1} \cdots + \sum_{\vec{r}_1 \vec{k}_1} \cdots \right] U_{d\vec{k}}(t_2, t_0) + \cdots \quad (\text{A11})$$

In the WBL approximation this equation reduces to the form

$$\frac{\partial U_{d\vec{k}}(t, t_0)}{\partial t} = -C_2 \tilde{V}_{d\vec{k}}(t) + C_3 U_{d\vec{k}}(t, t_0), \quad (\text{A12})$$

with the solution

$$U_{d\vec{k}}(t, t_0) = -C_2 \int_{t_0}^t dt_1 \tilde{V}_{d\vec{k}}(t_1) \exp[-C_3(t-t_1)], \quad (\text{A13})$$

where $C_3 = \Gamma(4ix-3)/2(1+2x^2)$. Next, taking into account Eqs. (A9) and (A10) the function $U_{\vec{k}_1 \vec{k}_2}(t, t_0)$ can be written in terms of $U_{d\vec{k}_2}(t, t_0)$:

$$U_{\vec{k}_1 \vec{k}_2}(t, t_0) = \delta_{\vec{k}_1 \vec{k}_2} - C_2 \int_{t_0}^t dt_1 \tilde{V}_{\vec{k}_1 d}(t_1) U_{d\vec{k}_2}(t_1, t_0) - \frac{2V_{LR^X}}{1+2x^2} \int_{t_0}^t dt_1 e^{i(e_{\vec{k}_1} - e_{\vec{k}_2})(t_1 - t_0)}. \quad (\text{A14})$$

In order to calculate $U_{d\vec{q}}(t, t_0)$ we first write down the coupled set of equations [on the basis of Eq. (3)] satisfied by the functions $U_{d\vec{q}}(t, t_0)$, $U_{\vec{q}_1 \vec{q}_2}(t, t_0)$, $U_{\vec{r}\vec{q}}(t, t_0)$, and $U_{\vec{k}\vec{q}}(t, t_0)$. Inserting the formal solutions for the functions $U_{\vec{q}_1 \vec{q}_2}(t, t_0)$, $U_{\vec{r}\vec{q}}(t, t_0)$, and $U_{\vec{k}\vec{q}}(t, t_0)$ into the differential equation for the function $U_{d\vec{q}}(t, t_0)$ one obtains the derivative $\partial U_{d\vec{q}}(t, t_0)/\partial t$ expressed in terms of $U_{d\vec{q}}(t, t_0)$, $U_{\vec{k}\vec{q}}(t, t_0)$, $U_{\vec{q}_1 \vec{q}_2}(t, t_0)$, and $U_{\vec{r}\vec{q}}(t, t_0)$. Inserting again into this equation the formal solutions for the functions $U_{\vec{q}_1 \vec{q}_2}(t, t_0)$, $U_{\vec{r}\vec{q}}(t, t_0)$, and $U_{\vec{k}\vec{q}}(t, t_0)$, and repeating this process again and again, one obtains

$$\begin{aligned} \frac{\partial U_{d\vec{q}}(t, t_0)}{\partial t} = & -i \tilde{V}_{d\vec{q}}(t) + (-i)^2 \int_{t_0}^t dt_1 \sum_{\vec{k}_1} \tilde{V}_{d\vec{k}_1}(t) \tilde{V}_{\vec{k}_1 \vec{q}}(t_1) + (-i)^3 \int_{t_0}^t \int_{t_0}^{t_1} dt_1 dt_2 \left[\sum_{\vec{q}_1, \vec{k}_1} \tilde{V}_{d\vec{q}_1}(t) \tilde{V}_{\vec{q}_1 \vec{k}_1}(t_1) \tilde{V}_{\vec{k}_1 \vec{q}}(t_2) + \sum_{\vec{r}_1 \vec{k}_1} \cdots \right] \\ & + (-i)^4 \int_{t_0}^t \int_{t_0}^{t_1} \int_{t_0}^{t_2} dt_1 dt_2 dt_3 \left[\sum_{\vec{k}_1 \vec{q}_1 \vec{k}_2} \tilde{V}_{d\vec{k}_1}(t) \tilde{V}_{\vec{k}_1 \vec{q}_1}(t_1) \tilde{V}_{\vec{q}_1 \vec{k}_2}(t_2) \tilde{V}_{\vec{k}_2 \vec{q}}(t_3) + \sum_{\vec{k}_1 \vec{r}_1 \vec{k}_2} \cdots + \cdots \right] + \cdots \\ & + (-i)^2 \int_{t_0}^t dt_1 \sum_{\vec{p}=\vec{k}_1, \vec{q}_1, \vec{r}_1} \tilde{V}_{d\vec{p}}(t) \tilde{V}_{\vec{p}d}(t_1) U_{d\vec{q}}(t_1, t_0) \\ & + (-i)^3 \int_{t_0}^t \int_{t_0}^{t_1} dt_1 dt_2 \left[\sum_{\vec{q}_1, \vec{k}_1} \tilde{V}_{d\vec{q}_1}(t) \tilde{V}_{\vec{q}_1 \vec{k}_1}(t_1) \tilde{V}_{\vec{k}_1 d}(t_2) + \sum_{\vec{r}_1 \vec{k}_1} \cdots + \sum_{\vec{k}_1 \vec{q}_1} \cdots + \sum_{\vec{k}_1 \vec{r}_1} \cdots \right] U_{d\vec{q}}(t_2, t_0) + \cdots \quad (\text{A15}) \end{aligned}$$

In the WBL approximation this equation is reduced to the following form:

$$\frac{\partial U_{d\vec{q}}(t, t_0)}{\partial t} = -C_4 \tilde{V}_{d\vec{q}}(t) + C_3 U_{d\vec{q}}(t, t_0), \quad (\text{A16})$$

where $C_4 = (1-x)/(1+2x^2)$ and has the solution as follows:

$$U_{d\vec{q}}(t, t_0) = -C_4 \int_{t_0}^t dt_1 \tilde{V}_{d\vec{q}}(t_1) \exp[-C_3^*(t-t_1)]. \quad (\text{A17})$$

The function $U_{d\vec{r}}(t, t_0)$ is identical with $U_{d\vec{q}}(t, t_0)$.

To calculate, e.g., the current $j_L(t)$, we still need the functions $U_{\vec{k}\vec{r}}(t, t_0)$ and $U_{\vec{k}\vec{q}}(t, t_0)$. The function $U_{\vec{k}\vec{r}}(t, t_0)$ can be obtained solving the set of the coupled differential equations for the functions $U_{d\vec{q}}(t, t_0)$, $U_{\vec{q}\vec{q}_1}(t, t_0)$, $U_{\vec{r}\vec{q}}(t, t_0)$, and $U_{\vec{k}\vec{q}}(t, t_0)$. Writing down the formal solution for $U_{\vec{k}\vec{q}}(t, t_0)$ and inserting into it, in the first step, the formal solutions for $U_{\vec{q}_1 \vec{q}_2}(t, t_0)$ and $U_{\vec{r}\vec{q}}(t, t_0)$ and, in the second step, the formal solutions for $U_{d\vec{q}}(t, t_0)$ and $U_{\vec{k}\vec{q}}(t, t_0)$, and so on, one obtains

$$\begin{aligned}
U_{\vec{k}\vec{q}}^{\vec{r}}(t, t_0) = & -i \int_{t_0}^t dt_1 \tilde{V}_{\vec{k}d}(t_1) U_{d\vec{q}}(t_1, t_0) \\
& + (-i)^2 \int_{t_0}^t dt_1 dt_2 \left[\sum_{\vec{q}_1} \tilde{V}_{\vec{k}\vec{q}_1}(t_1) \tilde{V}_{\vec{q}_1 d}(t_2) + \sum_{\vec{r}_1} \tilde{V}_{\vec{k}\vec{r}_1}(t_1) \tilde{V}_{\vec{r}_1 d}(t_2) \right] U_{d\vec{q}}(t_1, t_0) \\
& + (-i)^3 \int_{t_0}^t \int_{t_0}^{t_1} \int_{t_0}^{t_2} dt_1 dt_2 dt_3 \left[\sum_{\vec{q}_1, \vec{k}_1} \tilde{V}_{\vec{k}\vec{q}_1}(t_1) \tilde{V}_{\vec{q}_1 \vec{k}_1}(t_2) \tilde{V}_{\vec{k}_1 d}(t_3) + \sum_{\vec{r}_1} \dots \right] U_{d\vec{q}}(t_3, t_0) + \dots \\
& + (-i) \int_{t_0}^t dt_2 \tilde{V}_{\vec{k}\vec{q}}^{\vec{r}}(t_1, t_0) + (-i)^3 \int_{t_0}^t \int_{t_0}^{t_1} \int_{t_0}^{t_2} dt_1 dt_2 dt_3 \left[\sum_{\vec{q}_1, \vec{k}_1} \tilde{V}_{\vec{k}\vec{q}_1}(t_1) \tilde{V}_{\vec{q}_1 \vec{k}_1}(t_2) \tilde{V}_{\vec{k}_1 d}(t_3) + \sum_{\vec{r}_1} \dots \right] + \dots. \quad (\text{A18})
\end{aligned}$$

Under the WBL approximation this equation reduces to the form

$$U_{\vec{k}\vec{q}}^{\vec{r}}(t, t_0) = -C_2 \int_{t_0}^t dt_1 \tilde{V}_{\vec{k}d}(t_1) U_{d\vec{q}}(t_1, t_0) - \frac{i}{1+2x^2} \int_{t_0}^t dt_1 \tilde{V}_{\vec{k}\vec{q}}^{\vec{r}}(t_1), \quad (\text{A19})$$

where $U_{d\vec{q}}(t, t_0)$ is given in Eq. (A17). The function $U_{\vec{k}\vec{r}}^{\vec{r}}(t, t_0)$ has the identical form as $U_{\vec{k}\vec{q}}^{\vec{r}}(t, t_0)$.

*Electronic address: tomasz.kwapinski@umcs.lublin.pl

†Electronic address: taranko@tytan.umcs.lublin.pl

‡Electronic address: ewatara@tytan.umcs.lublin.pl

¹T. H. Oosterkamp, L. P. Kouwenhoven, A. E. A. Koolen, N. C. van der Vaart, and C. J. P. M. Harmans, Phys. Rev. Lett. **78**, 1536 (1997).

²Qing-feng Sun, Jian Wang, and Tsung-han Lin, Phys. Rev. B **58**, 13007 (1998).

³L. P. Kouwenhoven, S. Jauhar, J. Orenstein, P. L. McEuen, Y. Nagamune, J. Motohisa, and H. Sakaki, Phys. Rev. Lett. **73**, 3443 (1994).

⁴Qing-feng Sun and Tsung-han Lin, J. Phys.: Condens. Matter **9**, 3043 (1997).

⁵A.-P. Jauho, N. S. Wingreen, and Y. Meir, Phys. Rev. B **50**, 5528 (1994).

⁶B. R. Buřka and S. Lipiński, Phys. Rev. B **67**, 024404 (2003); B. R. Buřka and P. Stefański, Phys. Rev. Lett. **86**, 5128 (2001).

⁷R. Lopez, R. Aguado, G. Platero, and C. Tejedor, Phys. Rev. B **64**, 075319 (2001).

⁸Qing-feng Sun and Tsung-han Lin, J. Phys.: Condens. Matter **9**, 4875 (1998).

⁹G. Platero and R. Aguado, Phys. Rep. **395**, 1 (2004).

¹⁰J. König and Y. Gefen, Phys. Rev. B **65**, 045316 (2002).

¹¹W. Hofstetter, J. König, and H. Schoeller, Phys. Rev. Lett. **87**, 156803 (2001).

¹²G. Hackenbroich, Phys. Rep. **343**, 463 (2001).

¹³J. Göres, D. Goldhaber-Gordon, S. Heemeyer, M. A. Kastner, H. Shtrikman, D. Mahalu, and U. Meirav, Phys. Rev. B **62**, 2188 (2000).

¹⁴M. Plihal and J. W. Gadzuk, Phys. Rev. B **63**, 085404 (2001).

¹⁵L. Yi and J. S. Wang, Phys. Rev. B **63**, 073304 (2001).

¹⁶K. Kang, M. S. Choi, and S. Lee, Phys. Rev. B **71**, 045330 (2005).

¹⁷Y. Ji, M. Heiblum, D. Sprinzak, D. Mahalu, and H. Shtrikman, Science **290**, 779 (2000).

¹⁸S. Y. Cho, H. Q. Zhou, and R. H. McKenzie, Phys. Rev. B **68**, 125327 (2003).

¹⁹V. A. Margulis and H. A. Pyataev, J. Phys.: Condens. Matter **16**, 4315 (2004).

²⁰H.-K. Zhao, Phys. Lett. A **226**, 105 (1997); Z. Phys. B: Condens. Matter **102**, 415 (1997); Phys. Rev. B **63**, 205327 (2001).

²¹A. Cottet, W. Belzig, and C. Bruder, Phys. Rev. Lett. **92**, 206801 (2004).

²²Z. G. Zhu, G. Su, Q. R. Zheng, and B. Jin, Phys. Rev. B **70**, 174403 (2004), and references therein.

²³Qing-feng Sun and Hong Guo, Phys. Rev. B **64**, 153306 (2001).

²⁴E. Lebanon and A. Schiller, Phys. Rev. B **65**, 035308 (2001).

²⁵D. Sanchez and R. Lopez, Phys. Rev. B **71**, 035315 (2005).

²⁶R. Leturcq, D. Graf, T. Ihm, K. Ensslin, D. D. Driscoll, and A. C. Gossard, Europhys. Lett. **67**, 439 (2004).

²⁷M. Moskalets and M. Büttiker, Phys. Rev. B **70**, 245305 (2004); **69**, 205316 (2004).

²⁸S. Kohler, J. Lehmann, and P. Hänggi, Superlattices Microstruct. **34**, 419 (2003).

²⁹Z. Ma, Yu Zhu, Xin-Qi Li, Tsung-han Lin, and Zhao-Bin Su, Phys. Rev. B **69**, 045302 (2004).

³⁰M. Tsukada and N. Shima, in *Dynamical Processes and Ordering on Solid Surfaces*, edited by A. Yoshimori and M. Tsukada

- (Springer, Berlin, 1995), p. 34; S. Tsuneyuki, N. Shima, and M. Tsukada, Surf. Sci. **186**, 26 (1987).
- ³¹R. Taranko, T. Kwapiński, and E. Taranko, Phys. Rev. B **69**, 165306 (2004).
- ³²T. Kwapiński, R. Taranko, and E. Taranko, Phys. Rev. B **66**, 035315 (2002).
- ³³S. Camalet, S. Kohler, and P. Hänggi, Phys. Rev. B **70**, 155326 (2004).
- ³⁴M. H. Pedersen and M. Büttiker, Phys. Rev. B **58**, 12993 (1998).
- ³⁵Quin-feng Sun and Tsung-han Lin, Phys. Rev. B **56**, 3591 (1997).